POLYANILINE-BASED NANOCOMPOSITE STRAIN SENSORS

A Thesis

by

ZACHARY SOLOMON LEVIN

Submitted to the Office of Graduate Studies of
Texas A&M University
in partial fulfillment of the requirements for the degree of

MASTER OF SCIENCE

December 2011

Major Subject: Mechanical Engineering

Polyaniline-Based Nanocomposite Strain Sensors

POLYANILINE-BASED NANOCOMPOSITE STRAIN SENSORS

A Thesis

by

ZACHARY SOLOMON LEVIN

Submitted to the Office of Graduate Studies of
Texas A&M University
in partial fulfillment of the requirements for the degree of

MASTER OF SCIENCE

Approved by:

Chair of Committee,	Jaime C. Grunlan
Committee Members,	Abraham Clearfield
	Thomas Lalk
Head of Department,	Jerald Caton

December 2011

Major Subject: Mechanical Engineering

ABSTRACT

Polyaniline-Based Nanocomposite Strain Sensors.

(December 2011)

Zachary Solomon Levin, B.S., New Mexico State University

Chair of Committee: Dr. Jaime Grunlan

Health monitoring is an important field as small failures can build up and cause a catastrophic failure. Monitoring the health of a structure can be done by measuring the motion of the structure through the use of strain sensors. The limitations of current strain sensing technology; cost, size, form could be improved. This research intends to improve current strain sensing technology by creating a conductive polymer composite that can be used monitor health in structures. Conductive polymer composites are a viable candidate due to the low costs of manufacturing, tailorable mechanical and electrical properties, and uniform microstructure. This work will focus on determining if a all-polymer composite can be used as a strain sensor, and investigating the effects of filler, doping and latex effect the electrical and strain sensing properties.

Strain sensors were prepared from polyaniline (PANI)-latex composites, the morphology, mechanical, electrical and strain sensing properties were evaluated. These strain sensors were capable of repeatable measuring strain to 1% and able to measure strain until the substrates failure at 5% strain, with a sensitivity (measured by gauge factor) of between 6-8 (metal foil strain sensors have a gauge factor of 2). The best

performing strain sensor consisted of 4 wt.% polyaniline. This composition had the best combination of gauge factor, linearity, and signal stability.

Further experiments were conducting to see if improvements could be made by changing the polymer used for the matrix material, the molecular weight and the level of doping of the polyaniline. Results indicate through differences in strain sensing response; lower hysteresis and unrecoverable conductivity, that polyaniline latex composites can be adjusted to further improve their performance.

The polyaniline-latex composites were able to repeatable measure strain to 1%, as well as strain until failure and with gauge factor between 6-8, and a 70% increase in signal at failure. These properties make these composites viable candidates to monitor health in structures, buildings, bridges, and damns.

ACKNOWLEDGEMENTS

I appreciate the efforts and support of Dr. Jaime Grunlan for his guidance with research and this thesis, both of which would not have been accomplished without his input. I would like to thank my committee members, Dr. Clearfield and Dr. Lalk, for their guidance and knowledge which contributed to this research. I also thank Prof. Feller for his insights, ideas and expertise on strain sensing, and with whose collaboration this work came to be. I am also indebted to several people who helped me with the experimental portions of this work, especially Colin Robert, for help with the strain sensing tests, and our student workers, Jamie Wheeler, Katherine Sun, and Nicolas Ennesser. I am grateful for Christos Savva's assistance with Cryo-TEM and suggestions about nanoparticle features, and greatly appreciate the efforts of Dr. Hartwig and Robert Davidson for his help with this thesis.

TABLE OF CONTENTS

CHAPTER Page

LIST OF FIGURES

Page

Page

LIST OF TABLES

Page

CHAPTER I

INTRODUCTION AND LITERATURE REVIEW

Introduction

The monitoring of strain can provide considerable information about not only the physical properties of materials, but also the status or integrity of complex structures like bridges, buildings, cars, and airplanes. The ability to determine strain is an important factor in verifying the operational limits of a material, which will lead to improvements in safety, efficiency, and performance. The most common strain sensor is a metal foil strain gauge, yet their use is limited to measuring strain in a single direction on rigid materials because of the load shielding caused when a more rigid strain sensor is used on a flexible material. Therefore there is a need to create a strain sensor that can be made inexpensively, measure strain in multiple directions, and be used on flexible materials such as textiles. The focus of this work is to determine if an all-polymer composite using polyaniline and latex can produce a strain sensing material.

This thesis is in the style of Carbon.

Thesis overview

Chapter I contains some background information on the three primary topics pertaining to this research: polymer composites, polyaniline (PANI), and strain sensors. Chapter II describes the research objectives. Chapter III presents the strain-sensing properties of PANI filled latex composites evaluating the effectiveness of the strain sensing concerning the hysteresis, noise, cyclic stability, and gauge factor. Chapter IV focuses on the influence of latex type, molecular weight of PANI, and doping level of PANI, on the strain sensing, glass-transition temperature, storage modulus, and electrical conductivity of the composites. Chapter V summarizes this flexible nanocomposite sensor work and presents some options for future research.

Literature review

To give the reader a adequate background on these research background covering several areas as interest are presented below. The areas are strain sensing, electrical conductive polymer composites, and polyaniline. The strain sensing section should provide the reader with basic concepts of strain sensing, terminology, methods and some information on other leading research. In the electrically conductive polymer composite section information on the formation of a segregated network, percolation and piezoresistance are covered. The section on polyaniline includes brief history, structure, synthesis methods, doping, and electron transport in polyaniline.

Strain sensing

Strain is the fractional change in length, area, or volume of a material [1-2]. Symbolically it is represented by ε, and commonly referred to as the change in length divided by the original length $\frac{\Delta l}{l}$. The measurement of strain can indicate the stresses acting on an object. Other common physical properties that are related to the measurement of strain are pressure, torque, force, or load applied to an object. One practical way to determine strain is using materials whose electrical properties predictably changed when strained. Conductivity is commonly used as it can be affected by change in dimensions, resistance or both. Typically a potential is applied across the sensor and the change in current is measured, this method can be used for both piezoelectric and piezoresistive materials. [2-3]. Other non electrical methods exist, for example, the differences in phase of polarized light caused by a strain, can be measured though the use of computers and the strain can be determined [4-5].

A sensor's ability to measure is determined by the resolution, noise, sensitivity, hysteresis, range, linearity, and accuracy of the signal [3, 6]. All of these factors are important a wide variety of measurements for example; intensity, pressure, and temperature. For this document I will define how they relate to strain sensing.

The resolution of a sensor is the smallest change displacement that can reliably produce a consistent response. The common metal foil strain gauges have a resolution as low as $6x10^{-6}$ ε. Noise is the random fluctuation in signal that can result from a number of sources depending on the sensor and application. The sensitivity referred to as the

gauge factor is a dimensionless quantity, being the change in the relative amplitude $AR = \frac{R}{Ro}$ (the resistance R normalized by the initial resistance R_o) with strain ϵ, $GF = \frac{AR}{\varepsilon}$,. Hysteresis refers to the path dependence of the signal, a signal with low hysteresis will produce the same signal at ever given state, and large hysteresis will produce a different value depending on the direction of loading. The range of sensor can vary depending of several factors like temperature and time, as well as material properties like thermal expansion, response time, and loss modulus. All these factors affect the accuracy of a strain sensor and should be optimized for the best results.

Strain sensors can be contact or non-contact, active or passive, and dynamic or static. Contact sensors are those that are in direct contact with the object of interest, whereas non-contact sensors are not. Neither approach can be used for all applications. A non-contact sensor includes those sensors that are used to measure capacitance, inductance, and magnetic field [7-9]. Non-contact sensors have the advantage of being free of hysteresis and able to quickly measure changing conditions such as high-frequency vibrations. Inductive and some magnetic sensors, however, cannot measure static loading, as the changing magnetic field produces the electrical signal. Contact sensors, such as metal foil resistance strain gauges, are capable of measuring static and dynamic loads, but not at the same response rate of non-contact sensors. This difference is caused by the stress that the gauge experiences. The deformation of a material is a time dependent process; and at high or low frequencies the mechanical behavior may be dramatically different, either viscous at low frequencies or elastic at high frequencies.

Non-contact sensors do not have this problem as they do not deform when the stress is applied.

Capacitance sensors are non-contact and are capable of measuring dynamic conditions [10-12]. Capacitance sensors detect the changing electrical field between two conductors with a dielectric material between them. For most applications, the amount of dielectric material, or the distance between conductors, directly affects the measured electric field. Other dielectric materials can be used, but air is the most common and this limits sensor use to clean environments. Any debris in the gap of the conductors will prevent accurate measurements due to an inconsistent dielectric material. Static measurements are possible because the electric field stays constant at a given separation between plates. The range of these sensors is ~100 μm with sensitivity around GF=1 as capacitance has direct inverse relationship with distance. Capacitance strain sensors also require many additional electronic components; signal conditioner and special software in order to get a usable signal.

Optical strain gauges use light interference to determine the strain by detecting the changes in interference from light reflected off a target. A photocell can determine the difference in brightness, through the use of a computer. Optical sensors can be used with both contact and non-contact devices. In the non-contact sensor, light from a laser is directed at a two-way mirror that allows half of the light to pass through [13]. The reflected light is directed at the object, whose displacement is unknown. The light is reflected off the object and through the two-way mirror, where it is combined with the unaffected beam to create a diffraction pattern detectable by photocell. Contact optical

sensors use fiber optic wires that are attached to the material of interest [14]. When light is reflected from the edges of a fiber optic wire, the path the light travels is longer than it would be with an unbent wire. This difference in length affects the phase of the light emitted from the wire, altering the diffraction pattern. Optical sensors can be used in either dynamic or static environments, but they require a light source to operate and need precise alignment in order measure strain. Due to the high degree of precision required to maintain alignment of all the different optical components and the expense of those components make these sensors impracticable for real world applications.

A resistance strain gauge is a contact measurement device that does not have the fast response of a non-contact sensor. In gauges, some physical deformation of the sensing material takes place. In wire foil strain gauges, the changing dimensions of the metal film as well as the separation of the atoms result in a change in the electrical conductivity of the material [15-17]. The physical change in the material limits the dynamic response and causes hysteresis from the differences in deformation due to elongation and compression. The sensors studied in this thesis fall into this category.

Each sensor has limitations on the range of displacement it can be used to measure. For the non-contact sensors, their limits are determined by the strength of the magnetic or electric field. The field dissipates quickly, inversely proportional to the separation distance squared. For contact strain measurement devices, metal foil strain gauges or fiber optic sensors, the deformation must remain within the elastic range of deformation. If the amount of strain exceeds this limit, the material can fail and may not return to its original state when the stress is removed. It is currently very difficult to

measure the strain in flexible objects, those that can be bent, stretched, twisted etc., because commercial strain sensors only measure strain along one direction.

There is a role for a new kind of strain sensor, one that is inexpensive, flexible, and usable on a variety of materials. This sensor requires little phase lag, a reproducible hysteresis, dynamic and static response, and insensitivity to environmental factors. The applications for this sensor would be health monitoring of flexible materials, such as sails, parachutes, and clothing. Clothes capable of measuring the vitals of the wearer, parachutes able to indicate failure, and sails capable of determining the most efficient way to capture the wind could be developed with the use of this type of sensor [18-21] A polymer strain sensor, by its nature, is light, environmentally stable, and flexible. Additionally, polymers have many compatible properties with many textiles and could be integrated easily into their structure. The creation of these polymer-based strain sensors could be achieved by creating a polymer composite with piezoresistive behavior [22], which is the focus of the present work. Combining an electrically conductive polymer with an insulating matrix is expected to produce the desired properties for this new kind of sensor.

Other research is being conducted on strain sensing with a variety of materials. A brief description of some of these are listed in Table 1 below with materials used, the structure of those material the gauge factor and the strain range listed. Many of these sensors have exceptional performance; however there is always a tradeoff between performance and cost.

Table 1. Brief summary of experimental and commercial strain sensors.

Material	Form	Gauge Factor	Strain Range	Application	Notes
Metal Foil [23]	Geometric arrangement on polymer substrate	2	3%	Rigid materials, metals, ceramics, composites	Most common commercial strain sensor
Carbon Black-SBS copolymer [18]	Conductive polymer Composite on textile	31 80	<15% >15% -Failure	Textiles	27.6% filler Different gauge factors depending on strain <15% ε
Shape Memory Alloys [24]	Wire	3.42	8.0%	Buildings	Cost of SMA
ZnO [25]	Fine Wire	1200	1%	Biomedical, MEMS	Complex Assembly
Fe,Cu,Nb,B and SI alloy [26]	Commercial Magnetic Ribbon	175	1%	Non-contact	Use FFT to analyze signal, Magnetic field strength α Strain
Carbon Black, Carbon Fiber, Cement [27]	Concrete Beams composite	138	0.002%	Smart Materials Health Monitoring	Compressive Strain only
Bragg Grating [28]	Laser and Bragg Grading Reflector System	1.2	.0025%	Static and dynamic strains High Resolution	Small Strains

Electrically conductive polymer composites

To produce conductive polymer composites, a polymer is mixed with conductive filler to create an electrically conductive material that retains the polymer's physical characteristics. Typical fillers include carbon black, metal particles, or carbon nanotubes

[29-33]. The conductivity, σ, of the composite typically obeys a power-law relationship as a function of filler concentration, as expressed by [34-36].

$$\sigma = \sigma_0 (V - V_c)^n \quad (1)$$

where σ is the total conductivity of the material (Siemens/cm), V is the volume fraction of the conductive filler, V_c is the fraction of filler at the percolation threshold (point at which first continuous pathway of filler forms), σ_0 is the effective conductivity of the filler in the matrix, and n is the power law exponent. Percolation theory which describes how randomly distributed particles will form an interconnected pathway with increasing concentration, the effect on electrical conductivity is illustrated in Figure 1.

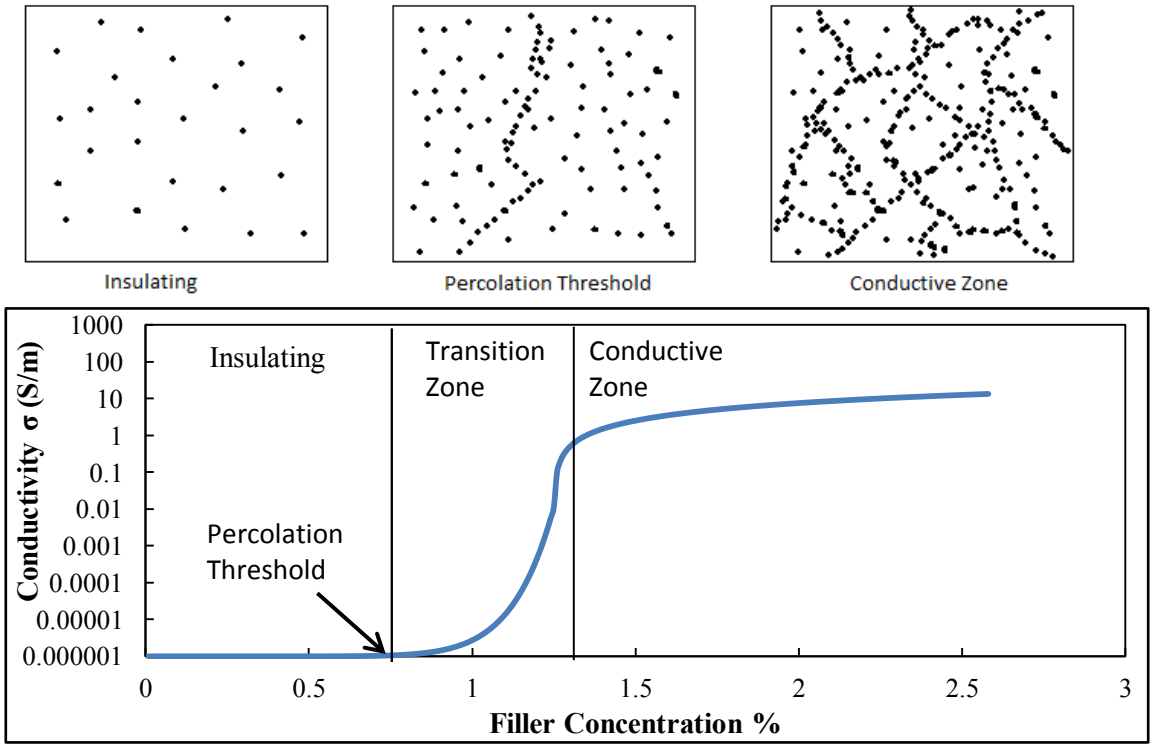

Figure 1. Schematic showing the formation of a percolating network with increasing filler volume with graph illustrating the effect of filler content on electrical conductivity.

Conductivity of polymer composites falls into three regions: insulating, transition, and conductive [31, 37-38]. In the insulating zone, the filler is of such a low concentration that very few particles are sufficiently close to allow electrons to tunnel (referring to quantum tunneling) between particles preventing electrons from being transported across the material. This behavior changes at the percolation threshold where the first conductive pathway forms through the material, this pathway is formed when enough particles are close enough to allow electrons to pass though the material. After the percolation threshold, the material is described as being in the transition region. In the transition region the number of conductive pathways increases, causing an order of magnitude rise in conductivity over a small increase in concentration. When the ratio of new conductive pathways to existing conductive pathways is small and the conductivity no longer increases dramatically with increase volume of filler, the composite is in the conductive zone.

In solution processed composites, the arrangement of conductive filler and matrix are random, limiting the conductivity of these composites. By forming a segregated network inside a composite, the conductivity at a given amount of filler is increased and the percolation threshold is lowered. A way to create a segregated network is to combine a suspension of conductive material and a suspension of polymers. The suspended polymer commonly used is referred to as latex, or polymer emulsion. This is combined with a conductive filler suspended in liquid which when dried can form a segregated network illustrated in Figure 2 [38].

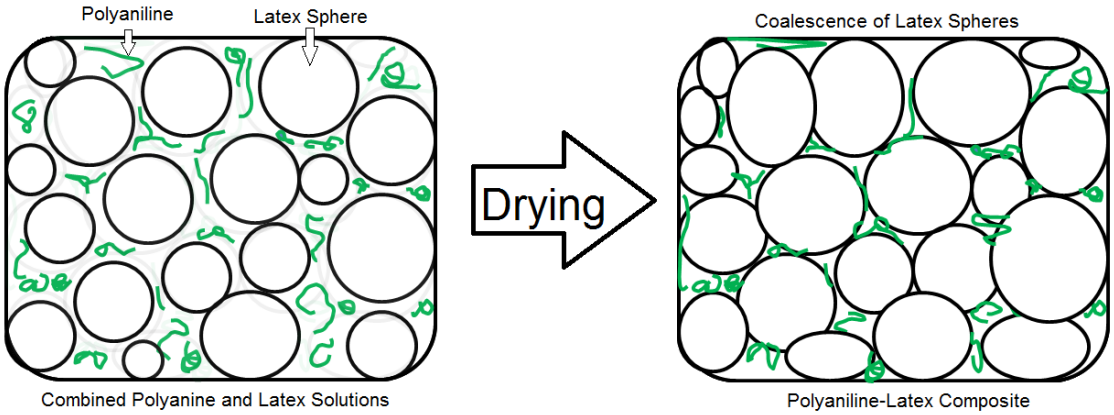

Figure 2. Mixture of latex and polyaniline solutions dried to form a segregated network composite.

During the drying process, the conductive filler is forced into the interstitial positions around the latex spheres. The volume occupied by the latex particles reduces the available space for the conductive filler to occupy, increasing the local concentration, which decreases the percolation threshold for the entire composite [31, 38-39].

Resistance and strain

If a material is deformed and its electrical properties change, typically resistance, it could be possible to measure strain. The most common materials used are thin metal films, but piezoelectric materials are also used [24]. A new area of research is in the use of polymers for strain sensing. In conductive polymer composites, this change in resistance occurs most dramatically near the percolation threshold because of the delicate network of conductive filler [29, 40-44]. This is due to the limited number of

pathways available to carry electrons so the loss of a few reduces the total available by a large fraction. The main factors that affect the resistance and strain response are the packing of the conductive filler and its intrinsic conductivity inside the matrix. Not only is intrinsic conductivity of the filler important, but also the effective conductivity of the filler in the matrix. Conductivity is affected by the interfaces between the filler particles. Near the percolation threshold, any variation in the distance between the conductive particles will impact the resistance of the composite [45-48]. When the material is elongated, the distance between filler particles increases, preventing electron tunneling, and disrupting conductive pathways pictured in Figure 3 [10, 20, 25, 49-52].

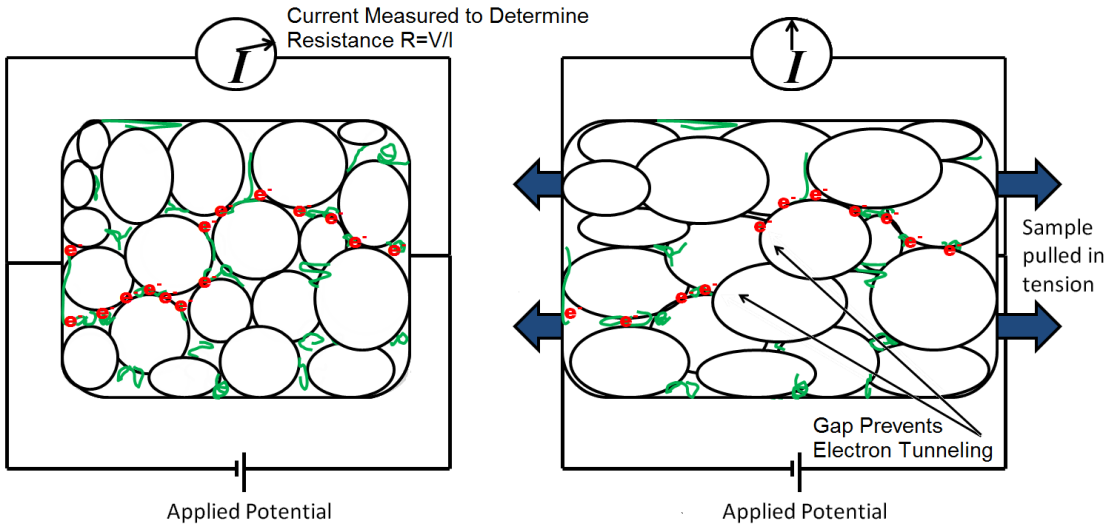

Figure 3. Illustration showing the effect of strain on composite's resistance.

Near the percolation threshold, the increase in resistance with decreasing filler concentration is dramatic and provides a large increase in resistance, as the material is strained. The electrical resistance R of a composite material can be modeled by [45]:

$$R = \left(\frac{L}{N}\right)\left(\frac{8\pi hs}{3a^2\gamma e^2}\right)\exp(\gamma s) \quad (2)$$

where L is the number of particles in a conducting path, N is the number of conducting paths, h *is* Plank's constant, s is the distance between conductive particles, a^2 is the effective cross section of electron tunneling, e *is* the charge of an electron, and γ is:

$$\gamma = \frac{4\pi(2m\emptyset)^{0.5}}{h} \quad (3)$$

where m is the electron mass and φ is the potential barrier between conductive particles. The variables that are related to concentration are s, N and L illustrated in Figure 4.

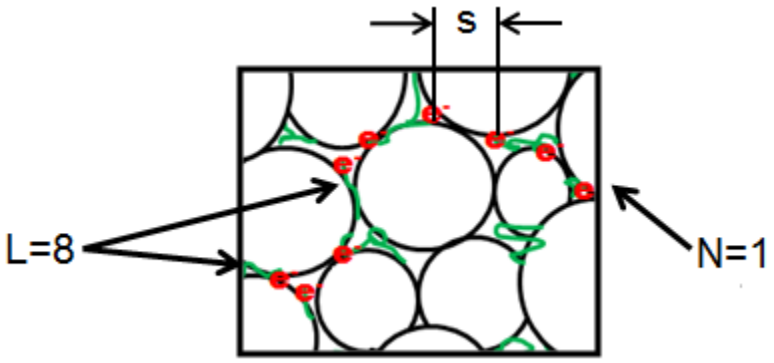

Figure 4. Illustration of factors affecting resistance in composites; ***s*** inter particle distance, ***N*** number of paths, and, ***L*** number of particles in path.

Using the proof found by Chen, P. F., the relationship between strain and resistance can be described by [45].

$$lnR = lnR_0 + ln\left[1 + \left(\frac{\Delta l}{l}\right)\right] + \gamma s_o\left(\frac{\Delta l}{l}\right) \quad (4)$$

Combining these equations the relationship between strain ε= ($\frac{\Delta l}{l}$) and the variables *s*, *L*, and *N* can be seen.

$$ln\left[\left(\frac{L}{N}\right)\left(\frac{8\pi hs}{3a^2\gamma e^2}\right)\exp(\gamma s)\right] = ln\left[\left(\frac{L_0}{N_0}\right)\left(\frac{8\pi hs_0}{3a^2\gamma e^2}\right)\exp(\gamma s_0)\right] + ln\left[1 + \left(\frac{\Delta l}{l}\right)\right] + \gamma s_o\left(\frac{\Delta l}{l}\right) \quad (5)$$

With these equations it is clear that the strain sensing is affected by the microstructure of the composite. The microstructure is influenced by; matrix material, aspect ratio of conductive particles, homogeneity of the composite structure, and the amount of filler.

Polyaniline

Intrinsically conductive polymers (ICPs) are a class of molecules that containing conjugated backbone (i.e., alternating double and single bonds) [53-55]. Since poly(acetylene) was first synthesized in 1977 by Shirakawa et al. [56], the number of new variations of ICPs have increased dramatically [53, 57-60]. Because these polymers combine some of the properties of both metals and polymers, they have many potential uses. ICPs are being studied for use in corrosion resistance, batteries, stealth coatings, electrochromic devices, inferred polarizers, LEDs, and sensors [54, 61-68]. One of the most popular and oldest known conductive polymers is polyaniline, which has been known since before the civil war [69].

Polyaniline (PANI) has been known about and studied since 1843, by Runge [70-72]. The PANI chemical structure contains an alternating benzene ring-like structure with nitrogen linkages, depicted in Figure 5. PANI can be yellow, green, blue, or violet

depending on the level of doping and electrical properties [73-75]. The synthesis, doping, mechanical, and electrical properties are discussed here, along with the mechanisms of its electrical conductivity. Depending on the doping method, PANI exists in several forms with different mechanical and physical properties [76-77].

Electrons are able to transfer along the polymer by continuous path that the hybridized sp^2 bonds create. The electrons are able to replace double bonds as they travel along the polymer depicted in Figure 5.

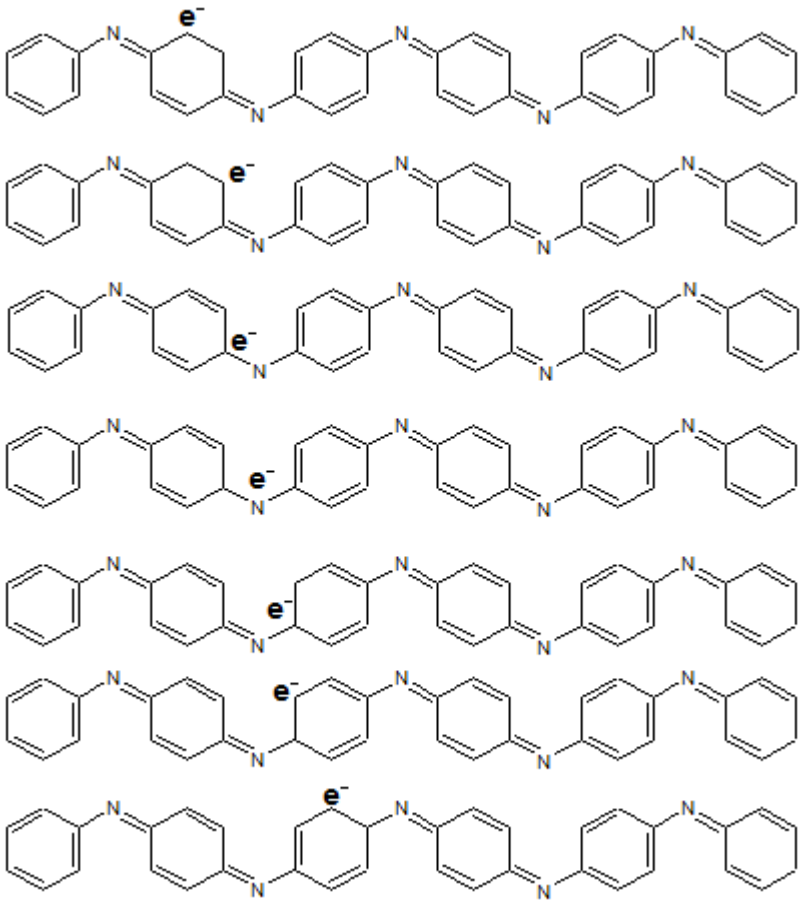

Figure 5. Electron transfer along oxidized polyaniline.

Synthesis of polyaniline

PANI can be synthesized from aniline by two methods, chemical or electrochemical [78-80]. In chemical synthesis, an oxidizing agent is used in an acidic medium to form the polymer. Common oxidizing agents are ammonium persulfate, ceric nitrate or ceric sulfate, and hydrogen peroxide or potassium bichromate [81-82]. The acidic medium used is usually hydrochloric or sulfuric acid with a pH between 0 and 2 [83-84]. For a variety of reasons, different stoichiometric ratios of oxidizing agent and aniline are used, that depend on the process selected, with some preferring stoichiometric lean, rich, or equivalent ratios of aniline and oxidant. This ratio can affect the final PANI product because a high concentration of oxidant can lead to polymer degradation.

Electrochemical synthesis is a process where a solution of aniline solvent and acid has a potential applied between 0.7 and 1.2 volts with a sweep rate between 10 and 100 (mV/s). The electrodes most commonly used are platinum because of it chemical stability, but other electrode materials can also be used [78, 85-88]. Other electrode materials include: metals [89-91], graphite [82, 92-94], transition metal salts [95], or semiconductors [96]. Electrochemical synthesis has benefits over chemical synthesis; (i.e., the products do not have to be separated from the initial solution), and characterization techniques like Raman spectroscopy are possible while the reaction is taking place [97-99].

Doping

PANI exists in two major forms. The first is the emeraldine base, which is insulating. Polyaniline is usually described as a combination of two different basic units, **A**, the reduced form of the repeat unit, having alternating benzene rings with nitrogen atoms in the following form:

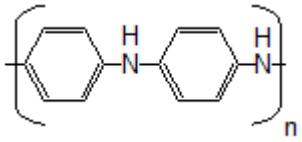

A

and **B**, the oxidized repeat unit, with one benzene ring alternating with a quinoid ring in the following form:

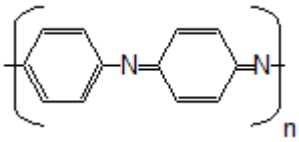

B

The combination of A and B are determined by the level of oxidation [100-102]. The emeraldine base form contains a combination of A and B. This form of deep blue PANI must be doped to become conductive. Doping lowers the potential barrier across the nitrogen atoms, by changing the bond angle.

The second form of PANI is the emeraldine salt, which is electrically conductive. The emeraldine salt has a deep-green color. The magnitude of electrical properties of PANI varies with the level of doping. The conductivity of PANI can vary from 10^{-10} (S/cm) for the emeraldine base, to 10 (S/cm) for the emeraldine salt [103-107].

Secondary doping of PANI can be accomplished by the addition of a polar acid such as hydrochloric acid. This adds hydrogen to the double-bonded nitrogen linkages in the back bone, the emeraldine salt can form different structures depending on syntheses and level of oxidation [108-110]:

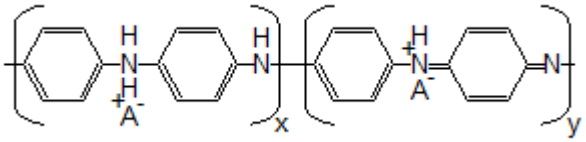

The quantity of the hydrogen bonds determines the level of doping or deprotination. Secondary doping forms a polysemiquinone radial cation, with "a half filled polaron conduction band", with a higher conductivity than unfilled quinoid ring [100, 111-112]. Conductivity of doped PANI is also increased by an increase in crystallinity, which occurs by the reorientation of molecules that is allowed by the uncoiling of chains from deprotination [113-116] . The hydrogen is supplied by adding strong acids, such as hydrochloric or sulfuric acid. PANI is most conductive above pH 4 and fully deprotienated when the pH is below zero [100, 117-118]. PANI, in it's doped from, has both the emeraldine base and emeraldine salt sections of the polymer chain. The amount of secondary doping is determined by the ratio of hydrogen atoms to nitrogen atoms in the back bone [119-120]. These linkages form "semiquinone radical cations" [84, 121-125], which directly affect the polymers conductivity. The number of electrons does not change with doping but the positive charge is localized on the nitrogen atoms. This creates a polaronic conduction band that transfers charge and makes the PANI conductive [126-131].

CHAPTER II

RESEARCH OBJECTIVES

A polymer based strain sensor using a conductive polymer composite could fill the need to inexpensively monitor the structural integrity of bridges, buildings and other structures. Making a conductive polymer composite is a complex task with many variables that can affect the final performance of the material, be this for EMF shielding, static dissipation, or strain sensing. These variables include the materials used (polymer matrix, filler, pH) but also include processing procedures, (filler stabilization, mixing, drying etc). Thus the amount of possible combinations and material properties are limitless. Therefore making a novel material requires establishing a procedure for a base system which can then be characterized, so comparisons can be made to relate other composites systems.

The objective of this research is to determine if a polyaniline-latex composite can be used to sense strain. The tasks necessary to complete this are determining the relationship between composition, electrical conductivity and strain sensing performance. Then the effects of changing the latex material, polyaniline molecular weight, and the doping for the polyaniline were studied, in order to determine their effect on conductivity and strain sensing performance.

Chapter III will focus on characterizing the electrical and strain sensing properties of a base polyaniline latex system, which will be evaluated as a strain sensor are used as a comparison for further experiments found in Chapter IV.

CHAPTER III

POLYANILINE-LATEX STRAIN SENSORS: SYNTHESIS, CHARACTERIZATION, RESULTS AND DISCUSSION

To create a polymer based composite strain sensor, the filler, matrix material and pH need to be considered. These variables can dramatically alter the mechanical, electrical, and strain sensing properties of the resulting strain sensing material sensitive material. The change in resistance with elongation was measured to determine strain sensing ability. Electrical conductivity of the final composite and viscosity measurements of the pre-solution were used to determine the percolation threshold, while microscopy using SEM reveal the microstructure, which provides insight to the mechanisms responsible for the pizoresistive behavior.

The main goal of this initial study is to develop a method for forming polyaniline latex composites with the correct piezoresistive behavior for use as a strain sensor.

Composite preparation

Polyaniline [Sigma Aldrich] with a molecular weight of either 5,000 or 50,000 g/mol was dissolved into dimethylacetamide (DMAC) [Sigma Aldrich] at a ratio of 1:50 PANI:DMAC by mass. The components were mixed at room temperature with a magnetic stir bar at 600 RPM. After the components were fully mixed, the solution was

stirred for an additional 5 minutes at 800 RPM. To remain consistent with the procedure from literature an initial dilute concentration of HCl was added followed by a more concentrated HCl solution, this was done in order to increase the concentration of polyaniline is solution [132]. The doping procedure is as follows: 0.1M HCl was added to the solution to achieve a ratio of 1:1.5 PANI: 0.1M HCl measured by mass. 1M HCl was then added a ratio of 1:1 to PANI mass. This mixture was then sonicated to disperse the polyaniline. Sonication was done using a Misonix XL-2000 with a 1/8-inch probe at a power level of 10, for 10 minutes in a water bath. The solution was then diluted 10 times and sonicated again. To reach the desired pH of either 3 or 2 a 1M HCL was added until the proper pH was reached. Once the solution had the desired pH, it was again sonicated for another 10 minutes. To make sure each composite presolution had the same pH the pH of the latex emulsions was adjusted to the deired level. For this Vinnapas 401 latex (PVAc copolymer) [Wacker] or Rovace 5140 [Rhom and Haas] latex was combined with 1M HCl until the desired pH was reached. To create the composites the PANI/DMAC/H_2O/HCl solution and pH-adjusted latex solution were combined and sonicated for 20 minutes, each precomposite solution had approximently 3.5 wt.% solids. After sonication, the solution was transferred via pipette to 3.5 cm diameter Petri dish bottoms, enough solution was added so that the final composites would have a mass of approximately 0.5 grams. The samples were then placed in a 55^{o}C oven and dried for an 48 hours, after which they were removed and placed in a vacuum desiccator for 24 hours.

Characterization

The homogeneity of the composites was evaluated using electrical conductivity measured with a Signatone four-point probe meter. A Keithley 2000 multimeter and Agilent DC power supply were used for measuring and generating voltage and current at values of 4 volts and 4 amps, respectively. Sample thickness was measured with a Mitutiy Absolute micrometer. To determine the homogeneity the conductivity was measured on the of the top and bottom surfaces and compared.

The percolation threshold was determined using a different homebuilt four point with variable resistance. A section measuring approximately 1/2 cm by 3 cm, was cut from the middle of the composite disk. Four lines were painted across the sample with silver paint. For samples greater than 2 wt.% PANI, a resistance setting of 4,680Ω was used, while samples with lower concentrations of PANI used a resistance setting of 1 MΩ. Samples below 2 wt.% were tested at both resistances with little effect on the results. The storage modulus at -65^{o}C, rubber modulus at 20^{o}C, and glass-transition temperature were determined by a Q800 series TA Instruments Dynamic Mechanical Analyzer (DMA). DMA measurements were performed with 1-Hz oscillation, 3^{o}C/min heating rate, and a preload tensile force of 0.01 N. The glass-transition temperature was determined by the peak in the loss modulus [133].

SEM images were taken with a Quanta 6000 series microscope. Samples were submerged in liquid nitrogen and then fractured to obtain a cross section for imaging. Fractured specimens were then sputter coated with 8 nm of platinum. The SEM was

operated at 13 kV accelerating voltage, 30-μs scan time, and a 3 spot size, estimated to be 1.2 nm. Rheological data were collected at room temperature using a TA Instruments AR G2, equipped with a parallel plate testing fixture, and using a shear-rate ramp from 1 to 1,000 s^{-1}.

Specimens were prepared for Cryo-TEM by applying 3 μl of aqueous precomposite mixture freshly glow-discharged C-Flat holey carbon grids and plunge-freezing using an FEI Vitrobot. Grids were transferred to a Gatan 626 cryo-holder and observed under low-dose conditions using an FEI Tecnai F20 TEM. Micrographs were recorded using a Gatan Ultrascan 1000 charge-coupled device (CCD) camera at calibrated magnifications.

Composite strain sensing was evaluated by attaching the PANI-Latex composites to beams of thermoset resin (EPOLAM 2020). The bulk EPOLAM was made using a vertical mold covered with Teflon (PTFE), with a 5 mm thick silicone gasket. Figure 6 shows the epoxy curing cycle and strain fixture setup. Substrate dimensions meet the ISO 527 standard of 100 × 10 × 4 mm, while composites were cut into 25 × 6 mm strips. Dry composites were 170-200 μm thick for standard samples and approximately 370 μm for thick samples. Substrates were cleaned using Loctite 770, a solution with aliphatic amine, the composite section was then attached to the center of substrate using Loctite 406 cyanoacrylate glue. Multifilament wires were placed on the 2.5mm from the edge of the composite strip, and covered with silver paint to remove contact resistance.

Tensile tests were performed with an Instron 5566A tensile machine. Clamps were attached to the last 20mm of the substrate. Testing was accomplished by cycling though a 1% strain four times and then strained until failure, at a strain rate of 2 mm/min. Deformation was measured with an extensometer. The stress and deformation were measured by the Instron software while the resistance was measured with a Picotest M3500A multimeter.

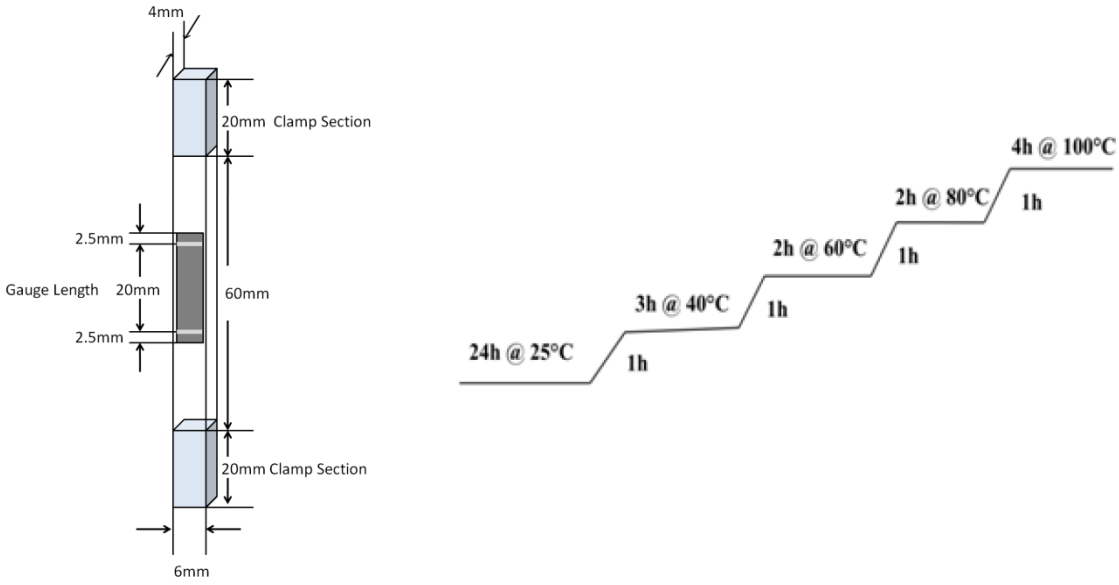

Figure 6. Epolam 2020 epoxy curing cycle and strain sensing apparatus made with Epolam substrate.

Polyaniline-poly(vinyl acetate) composite strain sensor

Structure

To examine if any interactions existed between the PANI and Latex spheres, pre-composite solution was examined with the use of a Cryogenic Transmission Electron Microscope (Cryo-TEM). These images shown in Figure 7, depict a 2 wt.% PANI solution used to make composites. It is clear that PANI collects around and between the latex particles. By comparing a neat pH adjusted PVAc solution with the same amount of DMAC (not shown), it was determined that the dark material around the latex spheres is PANI. In the solution, the PANI material only appeared at the surfaces of the latex spheres. This condition suggests that the PANI has a strong attraction to the latex, interrupting the normal formation of latex, noted by latex particles in intimate contact in the neat solution. The attraction is likely caused by the reduction in free surface area when material aggregates. The formation of PANI around the latex is the desired structure for the final composite because the PANI occupies the interstitial space forming a segregated network when dried.

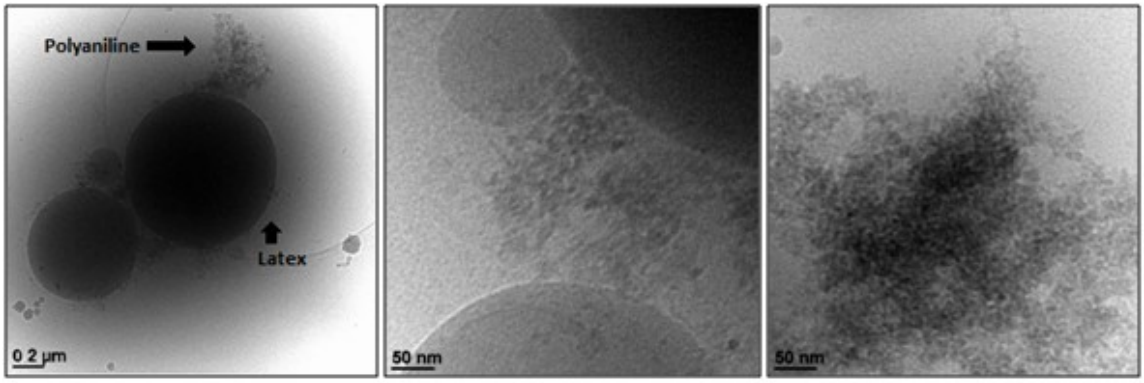

Figure 7. Cryo-TEM images of PVAc-latex 2 wt.% PANI solution.

To help understand how the PANI and the latex interact in the composites, samples were imaged with an SEM. Characteristic images of 4 wt.% samples are shown in Figure 8. Under low magnification, some PANI aggregates are seen inside the composite. These aggregates are separated by approximately 50 µm. Higher concentrations of these aggregates appear near the bottom surface of the composite. The bottom can be distinguished by the polymer strands that were generated when the sample was removed from the Petri dish. Four point probe testing determined that the composites were homogeneous. Under high magnification, the composite has a rough texture with lighter (brighter) areas indicating higher electrical conductivity (i.e., high PANI concentration). This rough-texture is consistent throughout the composite, which indicates that there is a homogeneous structure, with the PANI evenly dispersed. The resistance response is dependent on this even distribution of PANI in the latex. Areas of higher PANI concentration would remain conductive after elongation because the conductive filler would remain in intimate contact. A uniform PANI distribution also

ensures that the composite is free of large phases of differing PANI concentrations that could alter the mechanical and electrical properties.

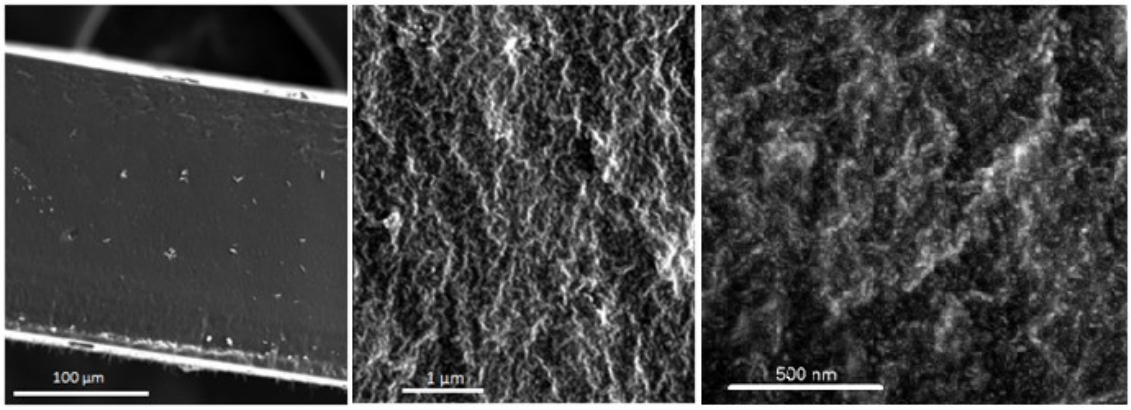

Figure 8. SEM images of 4 wt.% PANI-PVAc composites.

Mechanical properties

The mechanical and electrical properties are summarized in Table 2. Glass transition temperature is measured by the drop in storage modulus. The storage modulus does not follow any clear trend as the PANI content increases in the composites. This indicates that PANI is dispersed throughout forming a good composite with the latex. The trend in electrical resistance follows an expected power law trend.

Table 2. The properties of PANI-PVAc composites with PANI concentrations between 2 and 10 wt.%. "X"PANI-PVAc means "X" wt.% PANI in PVAc matrix.

Samples	PANI (wt.%)	PVAc (wt.%)	R 10^3 (kΩ)	σ (S/m)	T_g (^oC)	E @20^oC (MPa)
2PANI-PAVc	2	98	17.2	0.00	-0.9±4	40.0±16
3PANI-PAVc	3	97	45.9	0.10	-3.9±5	17.4±0.1
4PANI-PAVc	4	96	20.6	0.83	-2.4±2	29.4±4
5PANI-PAVc	5	95	20.6	2.68	-4.0±6	30.6±13
10PANI-PAVc	10	90	---	9.09	-2.8±5	34.2±45

Rheology

Rheological tests were performed on the aqueous pre-composite mixtures to determine a percolation threshold for the physical PANI network. The shear thinning behavior of the mixtures can be seen in Figure 9. All mixtures are 3.5 wt.% total solids. Figure 9(a) is the PVAc emulsion without any PANI and Figure 9(b) demonstrates the relative viscosity of the solutions used to create sample composites. Mixtures containing 1, and 1.5 wt.% PANI show a lower viscosity initially, this is due to the inclusion of DMAC solvent. The solvent decreases the viscosity and inhibits the formation of a network for the 1 wt.% solution and the 1.5 wt.% weight percent solution at low shear rate. At higher shear rates, the PANI particles create a network that raises the viscosity of the solution.

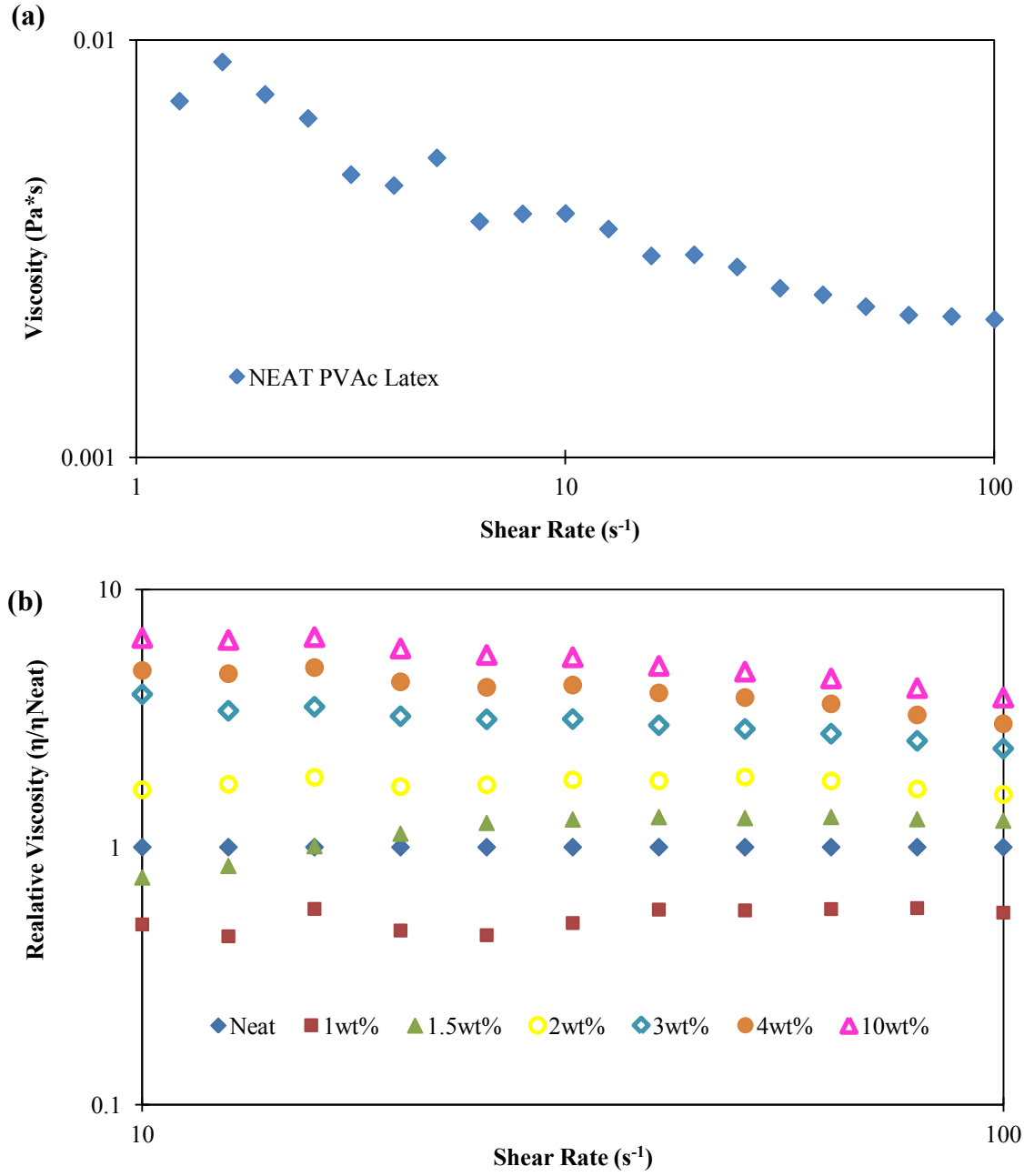

Figure 9. (a) Rheological behavior of neat Latex. (b) Neat normalized rheological behavior of PANI-PVAc precompsoite solutions.

Electrical percolation

Percolation was determined by fitting the power law relationship (Equation 1) to the electrical conductivity of PANI-PVAc composites as a function of PANI concentration, as shown in Figure 10. The rheological and electrical data show a similar percolation threshold with increasing PANI content. This relationship between viscosity and electrical conductivity has been observed by others [30, 44, 134-137]. The overlay of the rheological and electrical data provides two independent tests to confirm the percolation threshold. The reason both conductivity and viscosity are affected in the same manner is that both are controlled by the average distance between filler particles. By plotting the log of σ/σ_o against the log of V-Vc, and fitting a linear curve, the power law constants can be determined; as shown in Figures 10(b-c). Weight percent was used as a substitute for volume percent of filler because of the unknown density of the PANI after treating with solvent, doping, and drying at 55^{o}C. It is assumed, however, that the latex and PANI have similar densities, so volume and weight are nearly interchangeable.

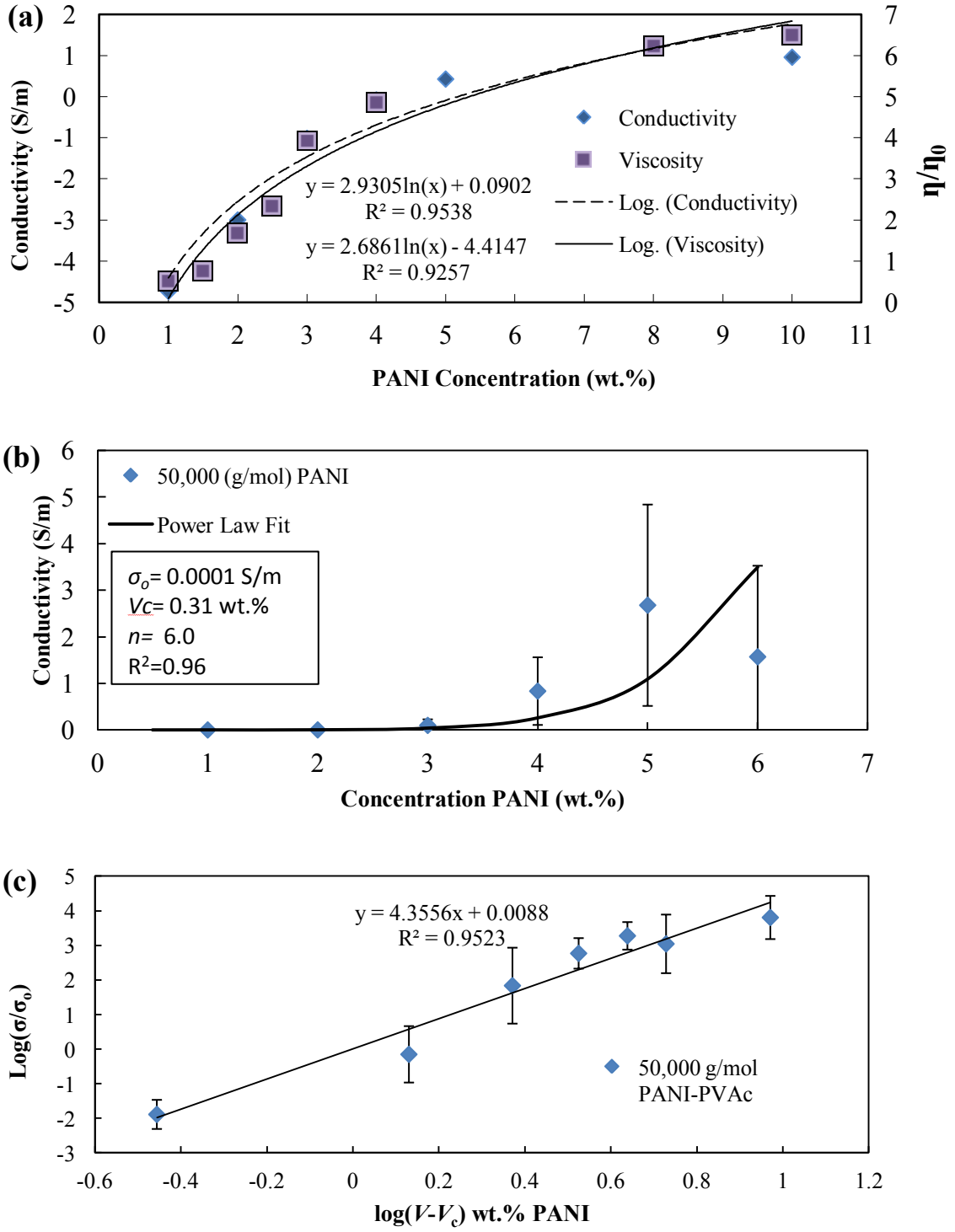

Figure 10. (a) Electrical conductivity and relative viscosity as a function of PANI concentration in a PANI- PVAc mixtures, showing agreement between rheological and electrical percolation. (b) Solid curve fit of electrical conductivity data to power law (Eq. 1) constants shown in insert. (c) Curve fit of $\log(\sigma/\sigma_o)$ and $\log(w\text{-}w_c)$ used to determine power law constants.

The conductivity behavior can be described by Equation 2. The factors that are affected by filler concentration are the pathway length (L), number of particles (N), and critical spacing between filler (s_0). It is assumed that the percolation threshold exists when $N = 1$ (138-139). For this condition, a critical threshold (L_c) and (s_0) must exist, and the resistance at percolation becomes (45):

$$R_p = \left(\frac{L_0}{1}\right)\beta s_0 \exp\left(\gamma s_0\right) \tag{5}$$

where the constant $\frac{8\pi h}{3a^2\gamma e^2}$ is represented by β. Filler loadings beyond this critical concentration contribute to all three components, (L, N, and s); but, the numbers of particles that contribute a single conductive path have some maximum value that will be near the critical value by virtue of the small distances between particles that allow for electron hopping to occur. Substituting these values into Equation 5, yields Equation 6, which describes the resistance, R_t, in the transition region of the percolation curve.

$$R_t = \left(\frac{L}{N}\right)\beta s \exp\left(\gamma s\right) \tag{6}$$

This equation describes the exponential behavior of the conductivity with increasing PANI filler, as conductivity is proportional to 1/R, as s dominates this equation. With additional loading of PANI, decreasing the distance between particles becomes more difficult and slows the decrease in resistance. The only mechanism to decrease resistance is the formation of new pathways, represented by N. Because this is a linear term, the decrease in resistance slows and electrical conductivity no longer increases in an exponential manner, which can be seen in Figure 10.

Strain sensing

From Equation 4, we can see the effect of strain on the resistance of the composite. The manner in which these composites sense strain is most likely due to the increasing resistance caused by the separation of PANI particles. As the composite is deformed, the separation between PANI particles increases and prevents electron hopping, as illustrated in Figure 3. The resistance response from these composites is determined by the way in which these PANI particles and the latex matrix respond to stress. When stress is applied to the material, the composite deforms accordingly and this stretching separates the PANI particles. When the distance between two particles reaches a critical level, electrons cannot tunnel and a barrier is created. As the number of these barriers increase, the number of conductive pathways decreases, which increases the resistance of the entire network.

These composites showed good resistance response to strain when compared to traditional metal foil gauges. The signal follows deformation and the stress applied closely, as shown in Figure 11(a). The 4 wt.% PANI composite became deformed with little mechanical resistance to the deformation of the substrate. The sharp peaks and low noise are also ideal for strain sensing because they give a clear indication of the state of strain. The effects of composition and thickness of the PANI-PVAc composites are shown in Figures 11(b) and (c). The change in relative resistance follows closely with the stress and strain. The peaks in the resistance are slightly out of phase with the stimulus, but the lag in response does not appear to be increasing with time. The initial

steep resistance increase to strain can be attributed to some rearrangement of the filler inside the composite matrix. The initial loading response seen here may indicate the behavior after some extended time, when the composite fully relaxes. In the present experiments, the remaining loading and unloading cycles stayed above the initial resistance value.

The signal quality improves with an increasing amount of PANI. When the resistance response of 3, 4, and 5 wt.% samples is compared, the trend shows that the signal quality increases with weight percent of PANI. The 3 wt.% sample had the largest degradation in signal with a drop of 35%, 4 wt.% the signal decreased 7%, and 5 wt.% the signal decayed 5%. The 5 wt.% PANI composites also show an increased sensitivity as noted by the general increase in amplitude 30% larger than 4wt% and 100% larger than 3 wt.%. Improvement in signal quality of the 5 wt.% samples can be attributed to the smaller distances between PANI particles that experience a more regular separation; however, an improvement in sensitivity does not occur. This lack of improvement could be due to a change in physical properties of the composite as the filler content increases. For instance, the samples become less tacky and more rigid with increasing PANI. One possible explanation for the improvement in strain sensing with 5 wt.% PANI is a change in Poisson's ratio between the 4 and 5 wt.% samples. Poisson's ratio would affect the way each composite was deformed in the direction normal to the applied stress. Three and 4 wt.% samples of PANI may contract more when stretched, allowing PANI particles to create new pathways as other pathways are disrupted, causing the

change in resistance to be less than predicted. The general behavior of the composites response along with strain and stress is depicted in Figure 11(a).

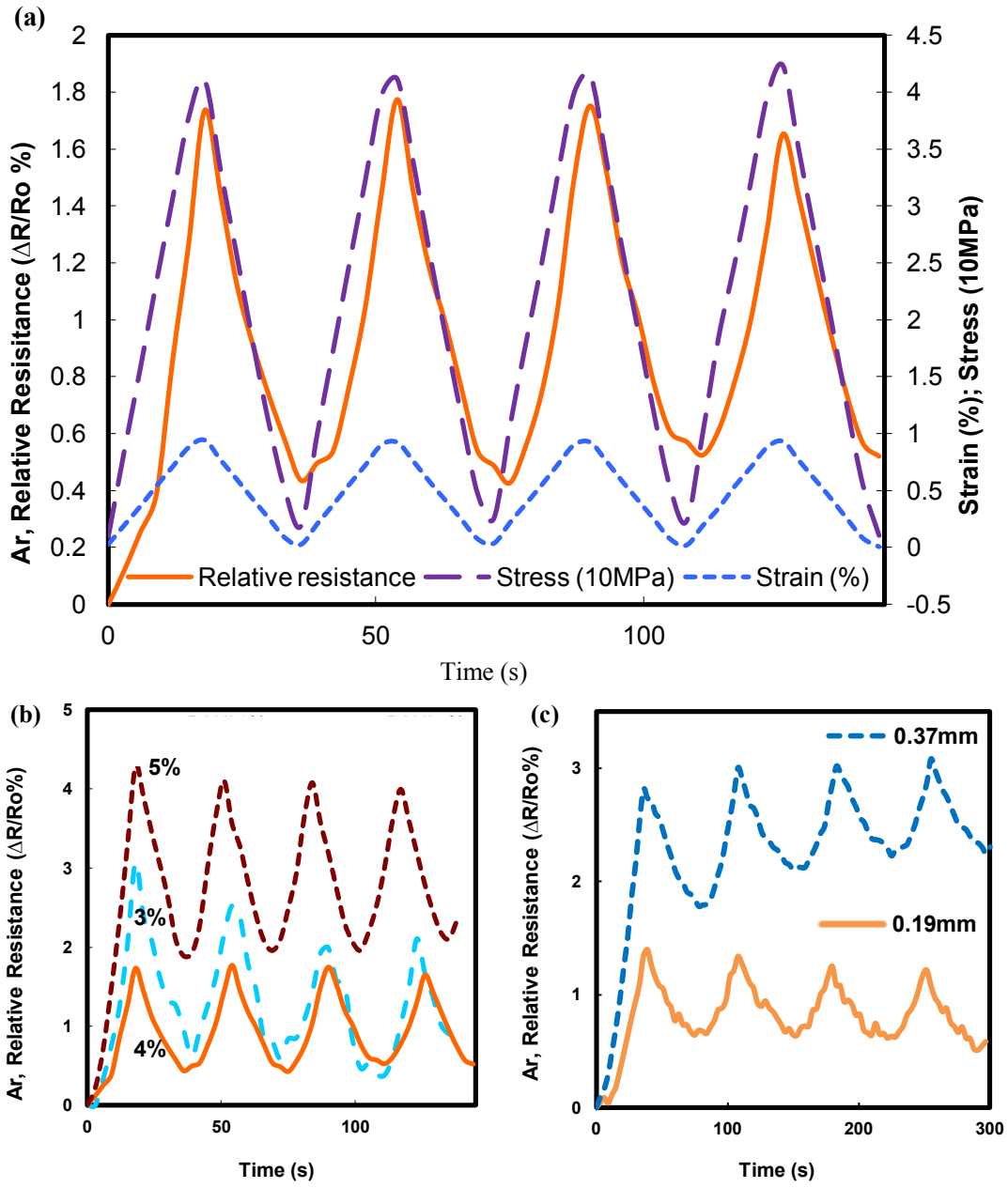

Figure 11. (a) Change in relative resistance of 4 wt.% PANI-PVAc composite, along with strain and cyclic loading stress; (b) Influence of PANI concentration on relative resistance for PVAc based composites. (c) Influence of thickness on strain sensing for 4 wt.% composites.

The response time of the 5 wt.% samples also shows an improvement over the 3 and 4 wt.% composites. The time delay in the peak resistance for 3 and 4 wt.% samples increases with each cycle, starting at approximately 3 seconds and increasing to 6 seconds (for the 3 wt.% sample) and 9 seconds (for the 4 wt.% sample). This increasing time delay is believed to be due to the more viscoelastic nature of the 3 and 4 wt.% samples (i.e. lower modulus). The energy dissipated during stretching may further soften the composites and increase the delay in resistance seen in figure 11(a). Two 4 wt.% samples were made at 0.370 mm and 0.190 mm thicknesses, to evaluate the influence of composite thickness on strain sensing. Thicker composites are more robust and could potentially be used for sensing compressive strain as well. The relative resistance response of these samples is shown in Figure 11(c). The thicker composite has a higher sensitivity, as evidence by the larger amplitude increase of over 100%, in both the initial increase in relative resistance and through each strain cycle. The thicker sample also exhibits less noise, which can be attributed to the greater robustness (i.e. less expansion when stretched).

By examining the location of the peaks in signal response, stress and strain it is possible to look at the signal time delay. For these PANI-Latex materials the signal response lagged by less than a second. This can be seen in Figure 12, where delay is clearly by the slight displacement in the relative resistance, stress, and strain data.

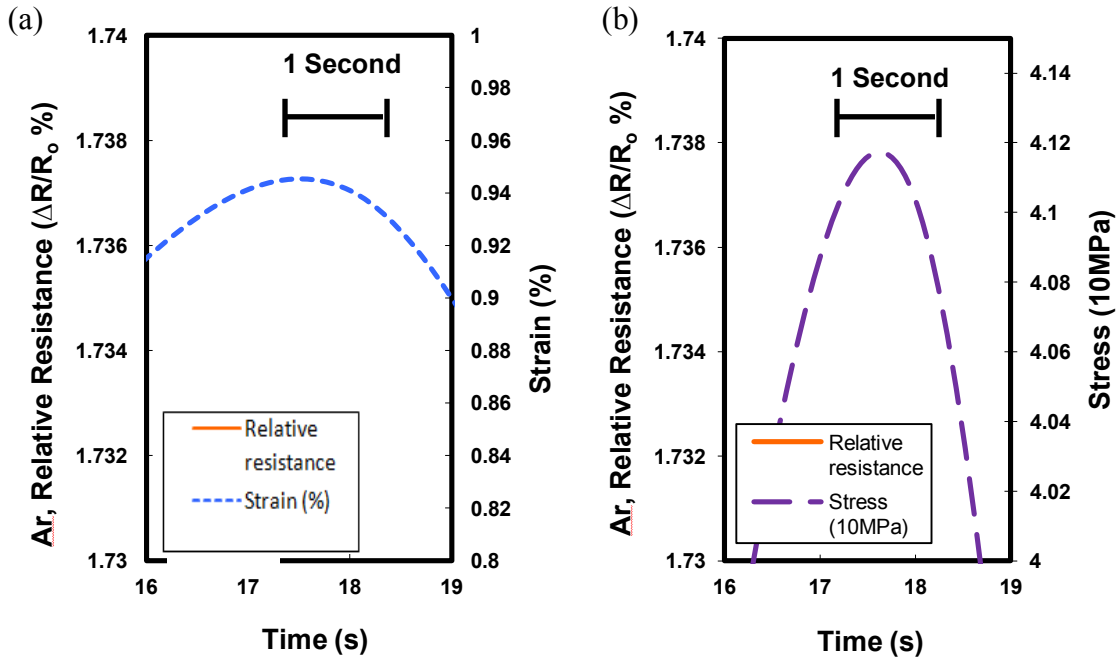

Figure 12. Comparison between the delay in signal response and strain (a) and signal and stress (b). Exhibiting a signal lag less than 1 seconds.

Figure 13 shows the change in relative resistance as a function of the percent strain, for repeated loading to 1% strain, for 3, 4, and 5 wt.% PANI-PVAc composites. The signal quality improves with increasing PANI content. The 4 wt.% PANI composite has the most constant signal and the 5 wt.% has the largest increase in resistance when strained. The amount of hysteresis between the 4 and 5 wt.% samples appears to be consistent amongst all three composites of each composition. This consistent signal indicates that the samples are able to recover well under cycling. The hysteresis is likely due to the way in which the latex responds to the applied stress (i.e., a viscoelastic manner due to the testing temperature being high relative to the glass-transition temperature and associated low elastic modulus). The viscoelastic nature of the matrix

material causes the composite to resist elongation initially, causing the near-parabolic resistance to increase initially. When the stress is reversed, the composite relaxes in a more linear manner and the resistance decreases accordingly.

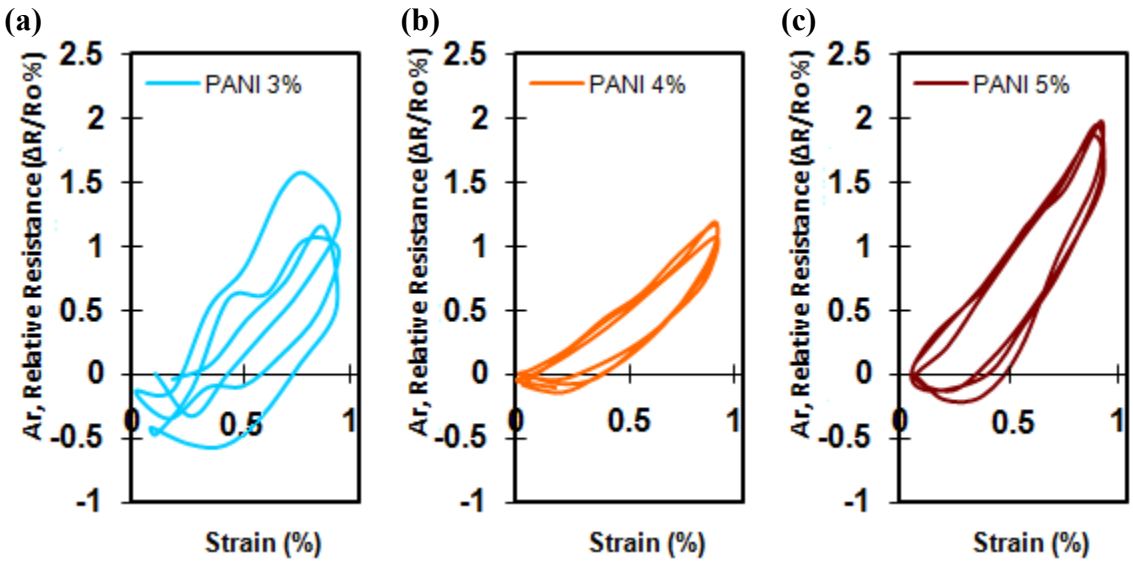

Figure 13. Relative resistance of (a) 3 wt.%, (b) 4 wt.%, and (c) 5 wt.% PANI-PVAc composites as a function of strain, to illustrate the fatigue response in PANI-latex composites.

These composites also show a near linear resistance response when elongated until failure, with a dramatic increase in resistance at failure, as illustrated in Figure 14(a). The gauge factors (i.e., slopes of the relative amplitude divided by strain until failure) for 3, 4, and 5 wt.% composites are shown in Figure 14(b). These PANI-PVAc composites show a near linear response to strain until failure and an abrupt increase in resistance at failure. The sharp peak in the relative resistance is due to failure of the substrate material. At failure, the sample is stretched to the point where the electrical

network is completely broken. The sudden large peak would be very useful in identifying when failure had occurred in these materials.

The gauge factor for all three PANI concentrations is better than a metal-foil strain gauge, which has a typical gauge factor of 2. Three and 4 wt.% PANI composites have a similar gauge factor (~6) and are within error of each other. The 5 wt.% composite has a gauge factor of eight, which is attributed to the greater stiffness associated with greater PANI content. In a metal foil strain gauge the path would be very linear with little hysteresis. At failure the signal would stop as the conductive material would fail breaking the circuit.

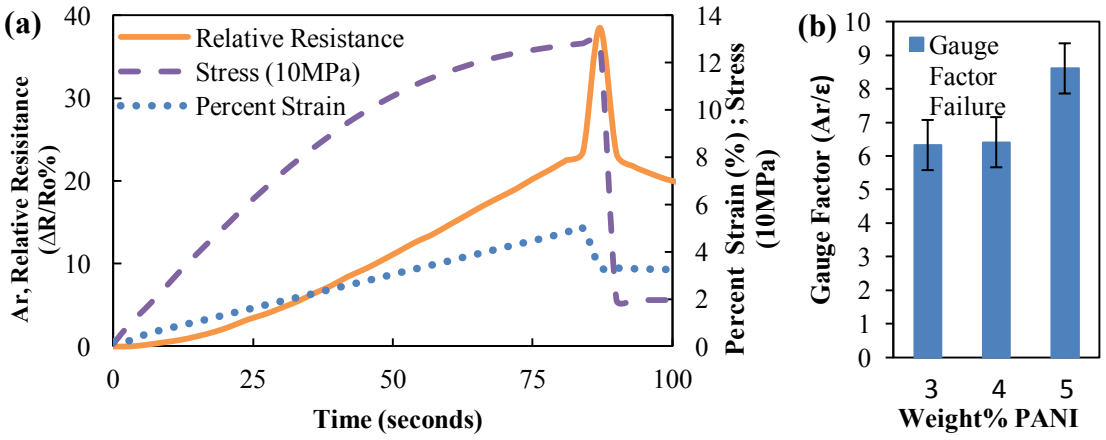

Figure 14. (a) Relative resistance, stress, and strain, as a function of time, for the 4 wt.% sample; (b) Gauge factors, for 3, 4, and 5 wt.% PANI-PVAc composites, for elongation until failure.

The strain sensing behavior could be altered the testing conditions. Increasing the temperature would likely increase the response delay and may also increase the ultimate ductility. An increase in temperature would soften the polymer matrix, increasing the viscous behavior. Lowering the temperature would likely cause the reverse but could lead to premature failure by making the composite brittle. Changing the strain rate may also change the signal response, high rate of test may produce a more linear response as the composite will deform more elastically, very slow may also produce a linear signal as the particle have time to reorient.

Conclusions

Polyaniline filled poly(vinyl acetate) composites with high gauge factor, and large ductility, and were fabricated. Three, 4 and 5 wt.% PANI samples showed the ability to sense strain under cyclic loading and linear resistance response when strained until failure. The quality of the signal increased with composite sensor thickness. These composites exhibit gauge factors between 6 and 8 A_r/ϵ, while traditional metal foil strain sensors gauge factors are closer to 2. SEM images demonstrate the homogeneity of the composite microstructure, while viscosity and electrical conductivity were used to determine the percolation threshold of these composites (Vc~0.26wt.% PANI). Chapter

IV evaluates the influence of PANI molecular weight, doping and polymer matrix modulus on strain sensing. These parameters can be used to further improve the sensing capability of these latex-based composites.

CHAPTER IV

INFLUENCE OF PANI MOLECULAR WEIGHT, LATEX MATRIX TYPE, AND DOPING ON STRAIN SENSING

The influence of the latex matrix modulus, molecular weight of polyaniline and doping level of polyaniline were evaluated in an effort to improve the strain sensing characteristics of PANI-latex composites. Strain testing was done under cyclic loading and compared to the baseline PANI-PVAc described in Chapter II. Electrical conductivity was used to determine percolation threshold, packing of particles, and effective intrinsic conductivity of PANI in the latex matrix. SEM images were used to visualize the composite microstructure. Composites were created using the procedure described in Chapter III, unless otherwise noted.

Influence of latex modulus

Rovace 5140 [Rohm and Haas], a vinyl acetate homopolymer was selected as an alternative matrix material for the PANI latex composites because it has a glass-transition temperature above room temperature (~30^{o}C). A sensor that has a glass-transition temperature above the testing temperature should have a decreased out-of-phase response and a more linear response because it will deform more elastically (i.e., exhibits glassy mechanical behavior). This favored for a strain sensor with a linear

resistance increase with strain. Figure 15 shows the change in resistance when a dynamic stress is applied to a 4 wt.% PANI-Rovace composite. This composite does not perform as well as the 4 wt.% PANI-PVAc (Fig. 11). The peaks associated with the maximum strain and deformation are sharp and in phase with the stress and strain, but the resistance response is noisy and completely out-of-phase (as well as decaying with each cycle), which makes this a poor strain sensor.

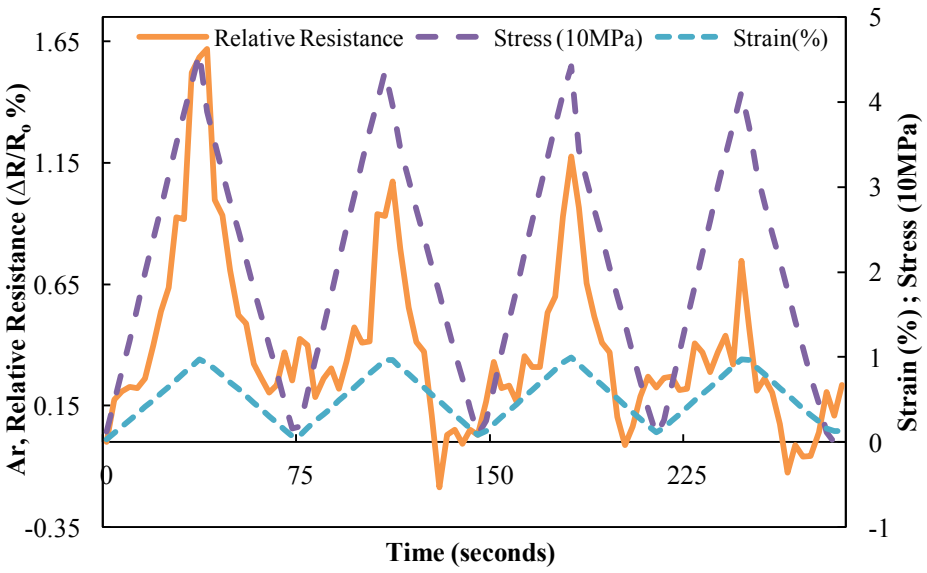

Figure 15. Relative resistance, stress and strain, as a function of time, for a 4 wt.% PANI-Rovace composite.

The difference in the resistance response, between Rovace and Vinnapas, can be partially explained by the difference in storage modulus (4500 MPa for Rovace and 25 MPa for Vinnapas). The higher storage modulus of Rovace is beneficial for the linearity it produces in the signal initially, but its glassy (brittle) nature also generates noise,

probably caused by deboning, or cracking that temporarily relieve stress. An out of phase response also exists seen at the end of each cycle, which is an unexpected behavior and would cause errors in detecting strain.

The Rovace-based composites deform in a more elastic manner than Vinnapas (PVAc) composites. Its highly elastic response improves linearity and decreases hysteresis of the signal. The change in relative resistance in the loading and unloading illustrates the hysteresis, shown in Figure 16. These composites have low hysteresis through the third cycle, which is an improvement over the PVAc composites that show distinctive parabolic loading and linear unloading response. Low hysteresis indicates a recoverable response that is good for strain-sensing applications. Despite this seemingly positive attribute, the general decay in resistance response is poor for these composites. Through each cycle, the amplitude decreases and the sensing ability becomes inconsistent. By the fourth cycle, the sample has almost no ability to sense strain and the signal is dominated by noise, with little response to the strain. The sensing instability is likely due to debonding of the sensor from the substrate and defects formed within the composite itself.

All components used in these experiments (epoxy substrate, adhesive, and composite sensor) are rigid in comparison with the PVAc-based sensor, so there is little ability to absorb energy. Instead, the composite separated from the substrate and the result is a poor signal. When the sensor is poorly bonded to the substrate, it does not deform along with the substrate and gives a false signal. The formation of cracks inside the composites may be cause of this signal decay, but this was not able to be proven

conclusively. There are several possible causes of these failures. High storage modulus at the testing temperature likely resulted in cracks forming as a means of stress relief. Defects and an inhomogeneous structure Rovace-based composite makes this problem worse because defects cause local stress concentrations and make failure more likely.

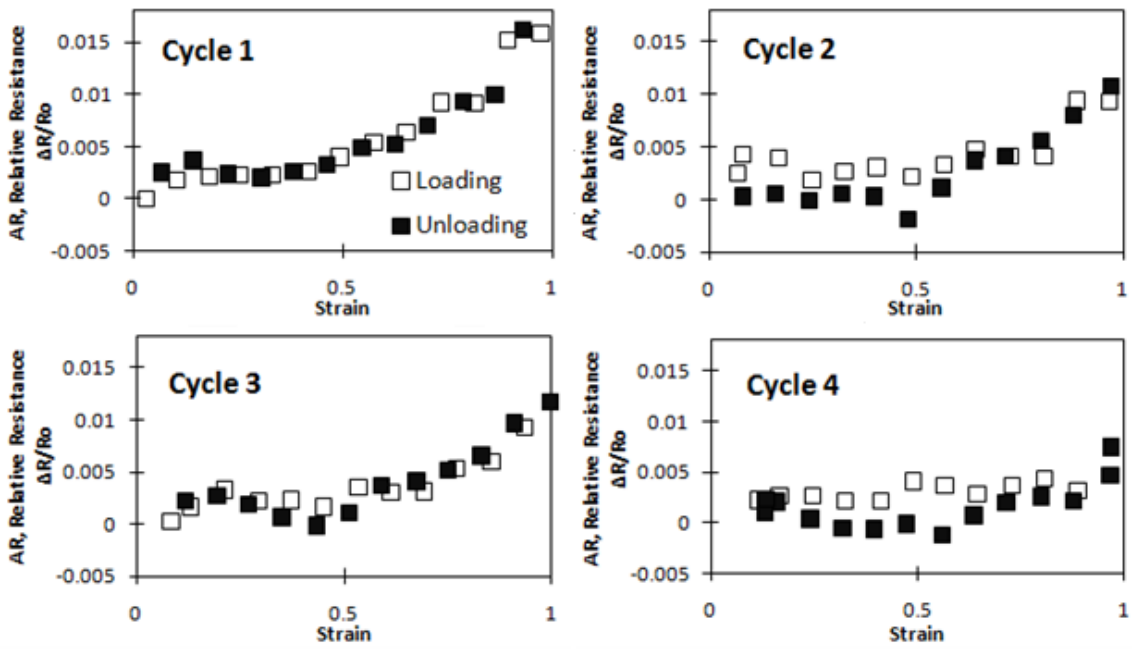

Figure 16. Loading and unloading relative resistance response to strain for 4 wt.% PANI-Rovace.

Influence of molecular weight of polyaniline

Figure 17 compares electrical conductivity of composites made with 5,000 or 50,000 g/mol PANI. Both systems have a similar percolation threshold, near 0.64 wt.%, PANI but the effective conductivity of the PANI differs by four orders of magnitude. Similarity in percolation threshold is the result of similar composite microstructure. At low concentration (<1 wt.%), PANI aggregates are similar in size and there are few interconnections between these aggregates, which create comparable percolation thresholds. It is believed that the higher molecular weight PANI creates more effective inter-aggregate connections at higher concentration. The relatively long chains of 50,000 g/mol PANI likely entangle with chains from neighboring aggregates, forming bridges that transport electrons across the composites. In composites containing 5,000 g/mol PANI, strong connections cannot form due to the smaller chain length. In this case, electrons have to tunnel across aggregates without the aid of intimately connected PANI bridges. We believe that the difference in the connections between PANI molecules and the effect that has on transporting electrons, causes difference in effective PANI conductivity (σ_o).

(a)

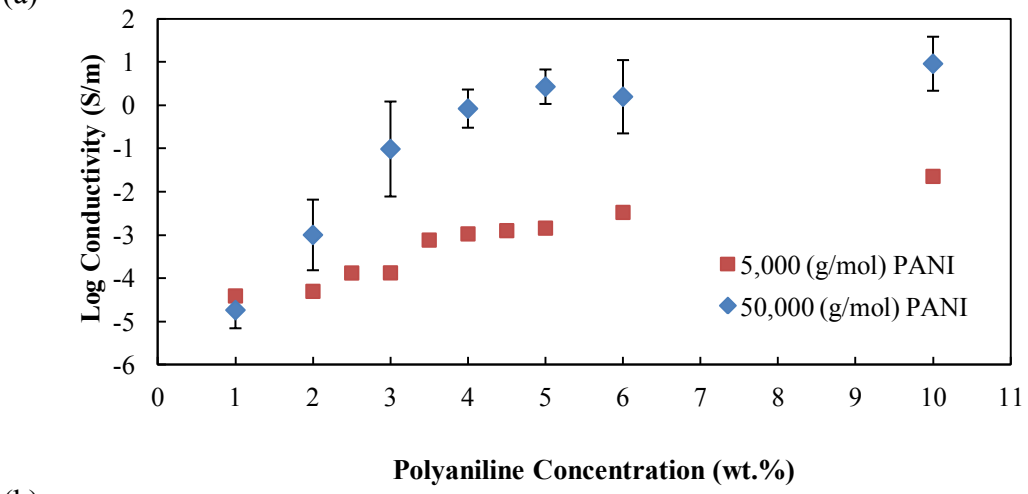

(b)

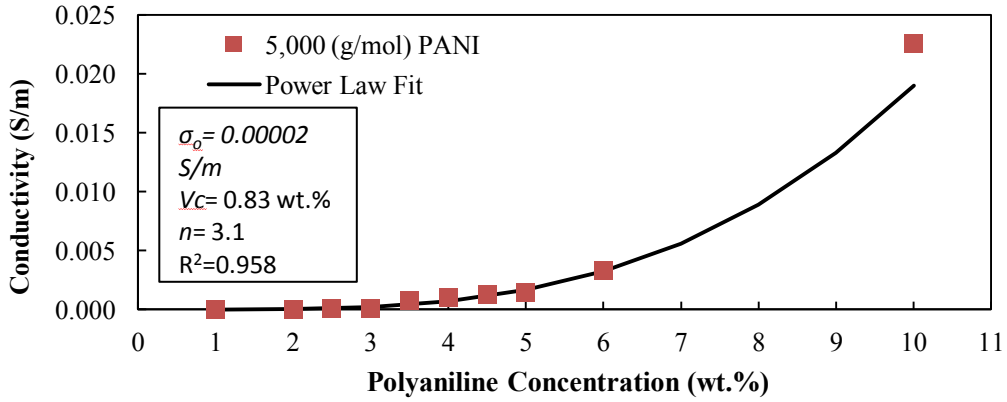

(c)

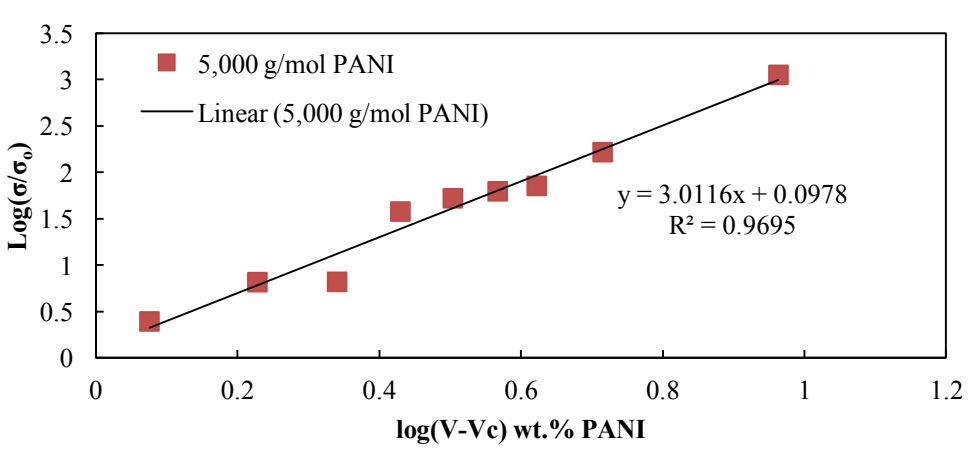

Figure 17. (a) Electrical conductivity of PANI-PVAc composites, with different molecular weight PANI, as a function of PANI concentration. (b) Overlay of conductivity data and theoretical data based on power law equation (c) Curve fitting used to determine power law constants for PANI-Rovace5140 composites.

Storage and loss modulus are very similar, within error, for both PANI systems, as shown in Figure 18(a). There is an initial increase in the storage modulus for both systems, at low PANI concentration, with an eventual leveling off beyond 2 wt.%, with a shear modulus of approximately 30 MPa. The 5,000 g/mol PANI-Latex series exhibits a higher storage modulus at 1, 3, and 4 wt.%. This may be due to higher packing density, greater packing density, or influence of a larger number of end groups in the lower molecular weight species. Loss modulus shows a similar pattern in Figure 18(b), with both series exhibiting the same values. Glass transition temperature Figure 18(c) also reflects this similarity. Filler concentration has little effect on the glass-transition temperature of the composites for either series, due to the segregation of filler in a latex-based composite (i.e., little interaction between matrix and filler) [140-141]. Any significant interaction between matrix and filler would result in a significant increase in Tg [142-143].

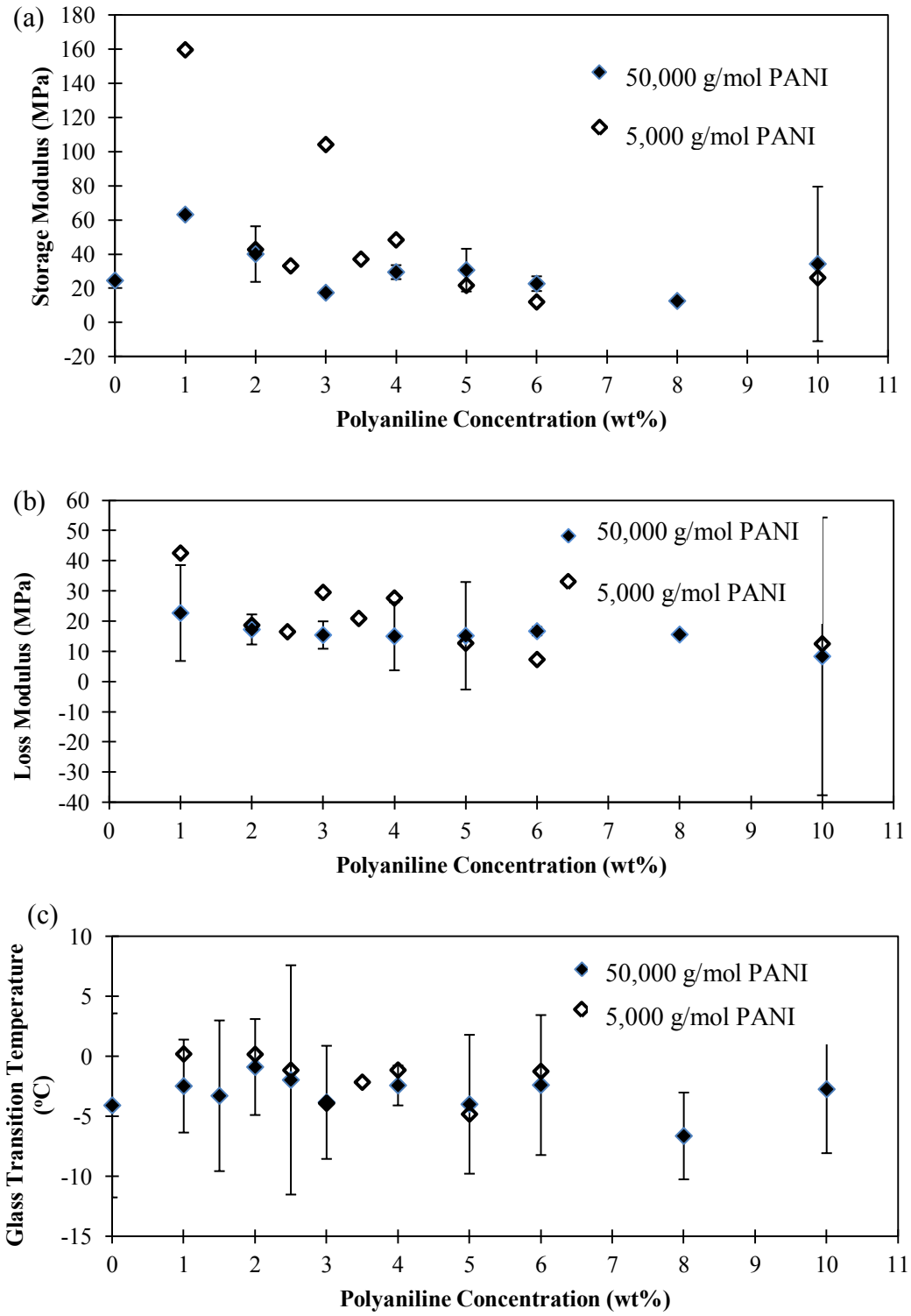

Figure 18. Storage (a) and loss modulus (b) at 20°C, and glass transition temperature (c) as a function of PANI concentration in PVAc latex-based composites.

Differences in PANI molecular weight are more noteworthy in the piezoresistive behavior of these composites. Figure 19 shows the relative resistance of 4 wt.% PANI samples under cyclic loading. Samples were alternately elongated at a rate of 3 mm/min to 1% strain, and then returned to starting position. The 5,000 g/mol sample shows a general increase in resistance under loading with little change when the stress is removed. This result suggests that the PANI particles are pulled further apart during stretching. Increased particle separation inhibits electrons from tunneling between them. The 50,000 g/mol sample shows a nearly in-phase recoverable response to the applied stress. There is slight amplitude decay as the cycling progresses, which is likely due to reorientation of the particles and a slight loss of entanglements between PANI chains and particles. Longer 50,000 g/mol PANI chains are better networked than 5,000 g/mol. When the composite is stretched, the polymer entanglements prevent the particles from separating too much. This strong network results in recoverable resistance and lower total resistance change during cycling. In 5,000 g/mol composites, the particles are isolated with few interconnections. The lack of any recovery in resistance indicates that these low molecular weight particles move apart and cannot return to their pre-stressed state.

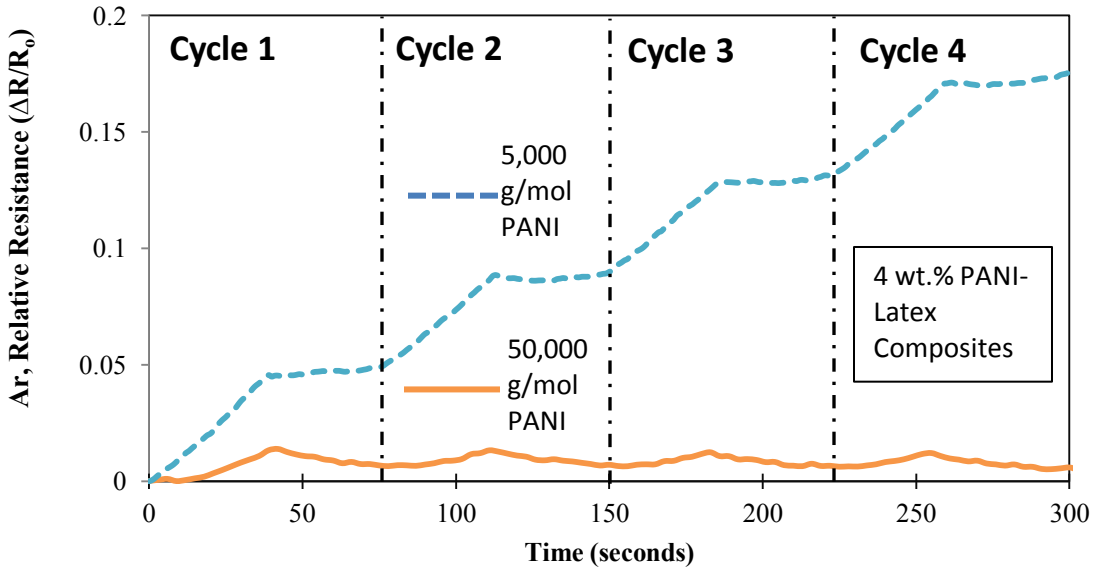

Figure 19. Relative resistance response of 4 wt.% PANI-PVAc composites as a function of time. Samples were alternately elongated at a rate of 3mm/min to 1% strain then returned to the starting position.

The effect concentration of PANI has on the sensing characteristic of the composites provides further evidence of the piezoresistive mechanisms involved. Figure 20 demonstrates the relative resistance of 5,000 g/mol PANI composites of varying PANI concentration. The resistance response appears to decreases as loading of PANI increases to 5 wt.% PANI, with additional PANI concentration the response seems to increase. This was not able to be confirmed by additional testing so no definite conclusions can be drawn. This result is expected for composites that are composed of discrete particles that form a segregated network in an insulating matrix. Near the percolation threshold, the distance between PANI particles is very near the critical separation where electrons can tunnel. With larger distances between particles, the elongation caused by strain disrupts the conductive network and the resistance increase

is larger. In composites with higher loadings of PANI, the particles are sufficiently close to each other such that, even with the same separation, they remain in closer contact and do not approach the critical distance for tunneling. The noise observed in the 5, 6, and 10 wt.% samples is believed due to the shifting PANI particles and decreasing thickness with elongation.

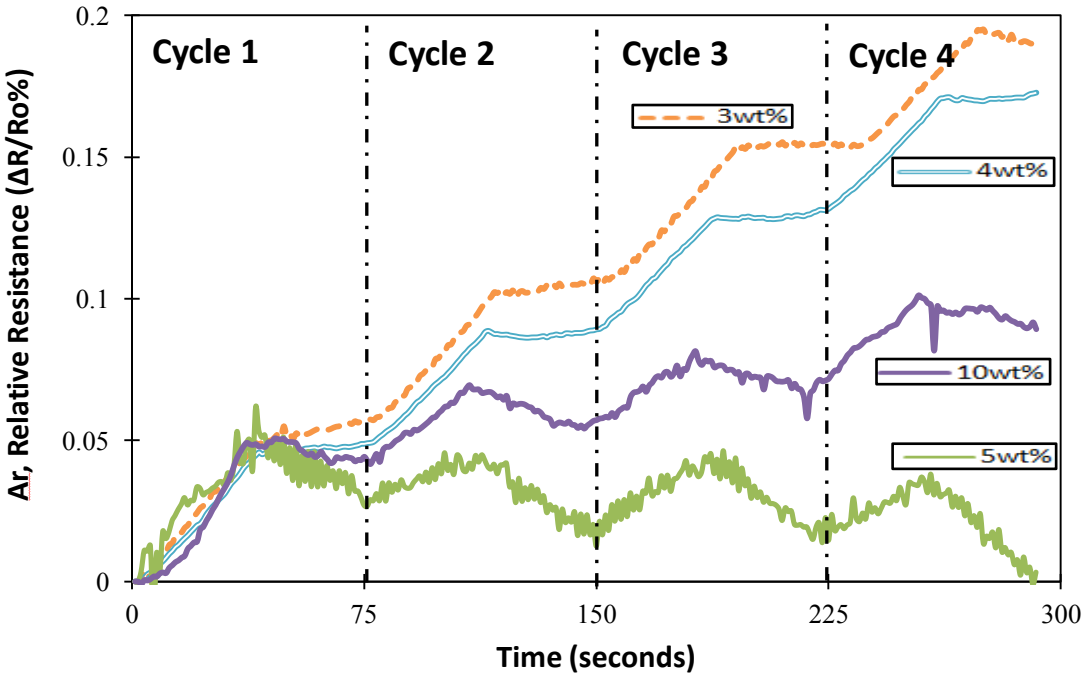

Figure 20. Relative resistance response of 5,000 g/mol PANI-PVAc composites with varying compositions. Samples were strained to 1% then released at a rate of 3 mm/min .

Figure 21 shows three different magnifications of the 5,000 g/mol PANI-PVAc composite cross-section. These images highlight the interconnected structure of this composite. At low magnification, the entire cross section of the 4 wt.% PANI composite

shows no aggregation or separation of particles at either surface. At higher magnification, the general structure can be seen with 20 nm light-colored spots that could be individual PANI particles. The segregated network is not visible due to the effects of DMAC on the composite during drying. The solvent softens the latex spheres, which causes them to coalesce into a homogeneous matrix.

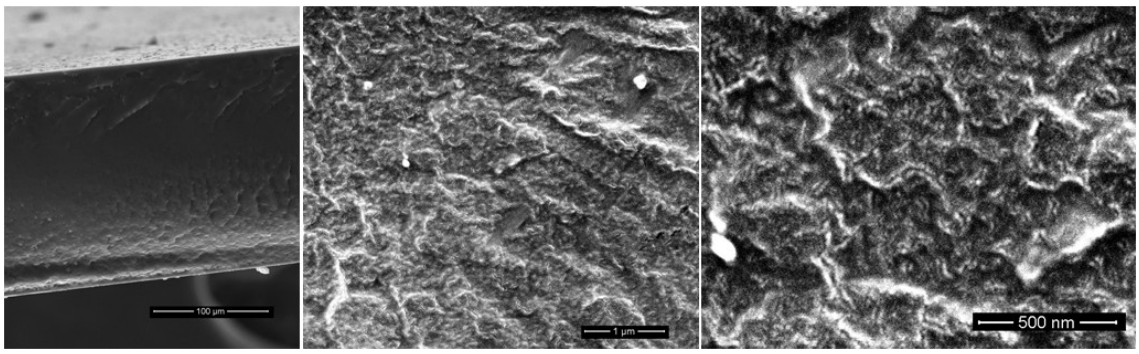

Figure 21. SEM Images of 4 wt.% 5,000 g/mol PANI-PVAc composite.

Effects of doping on polyaniline composites

Initially the electrical conductivity of the pH 2 composites is several orders of magnitude higher than pH 3 composites. This conductivity differential diminishes as the concentration of PANI increases. At the highest concentrations of PANI, the conductivity of the pH 2 series is essentially the same as the pH 3, as shown in Figure 22. The pH 2 series does not have error bars because only a limited amount of samples

were made, but, the difference in conductivities at the lowest concentrations is large enough to assume that the difference is significant.

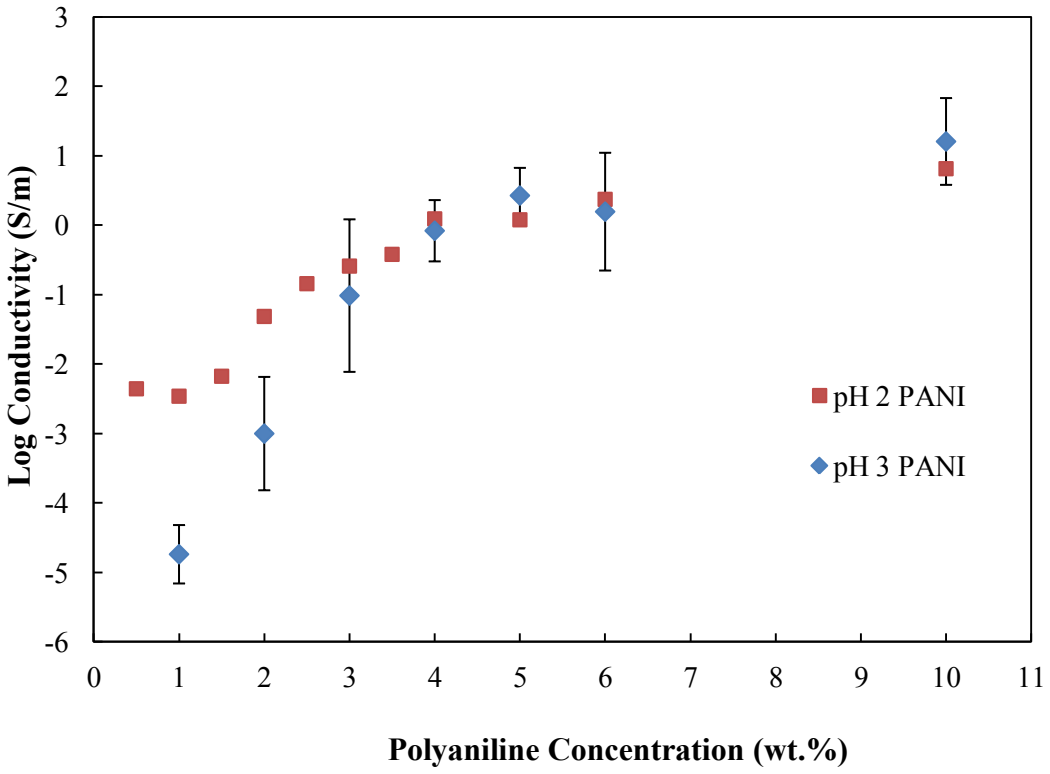

Figure 22. Electrical conductivity of PANI-PVAc composites, with pH of 2 and 3, error bars indicate the variation in different series of identical composites.

The percolation threshold, effective intrinsic conductivity, and geometric-packing terms, for these systems, are determined by plotting the log of relative conductivity as a function of log of weight percent minus the percolation threshold, as shown in Figure 23(a), Figure 23(b) the experimental and theoretical data are shown. The effective conductivity, percolation threshold and geometric packing factor for pH 2 samples are; 0.017 S/m, 0.51 wt%, and 2.8, while pH 3 parameters are; 0.0001 S/m, 0.26 wt%, and 6.2. All three factors are dependent not only on the intrinsic filler conductivity, but also on the microstructure of the composite and the filler. The orientation of the fillers can play a large role in the percolation threshold because the degree of dispersion and particle contacts are related. The size, shape, separation, and packing of the conductive filler have the greatest impact on the percolation threshold. The higher percolation threshold for the pH 2 series can be attributed to a different structure of PANI aggregate, or a phase separation of the PANI with latex, with different regions containing different concentrations of the conductive fillers.

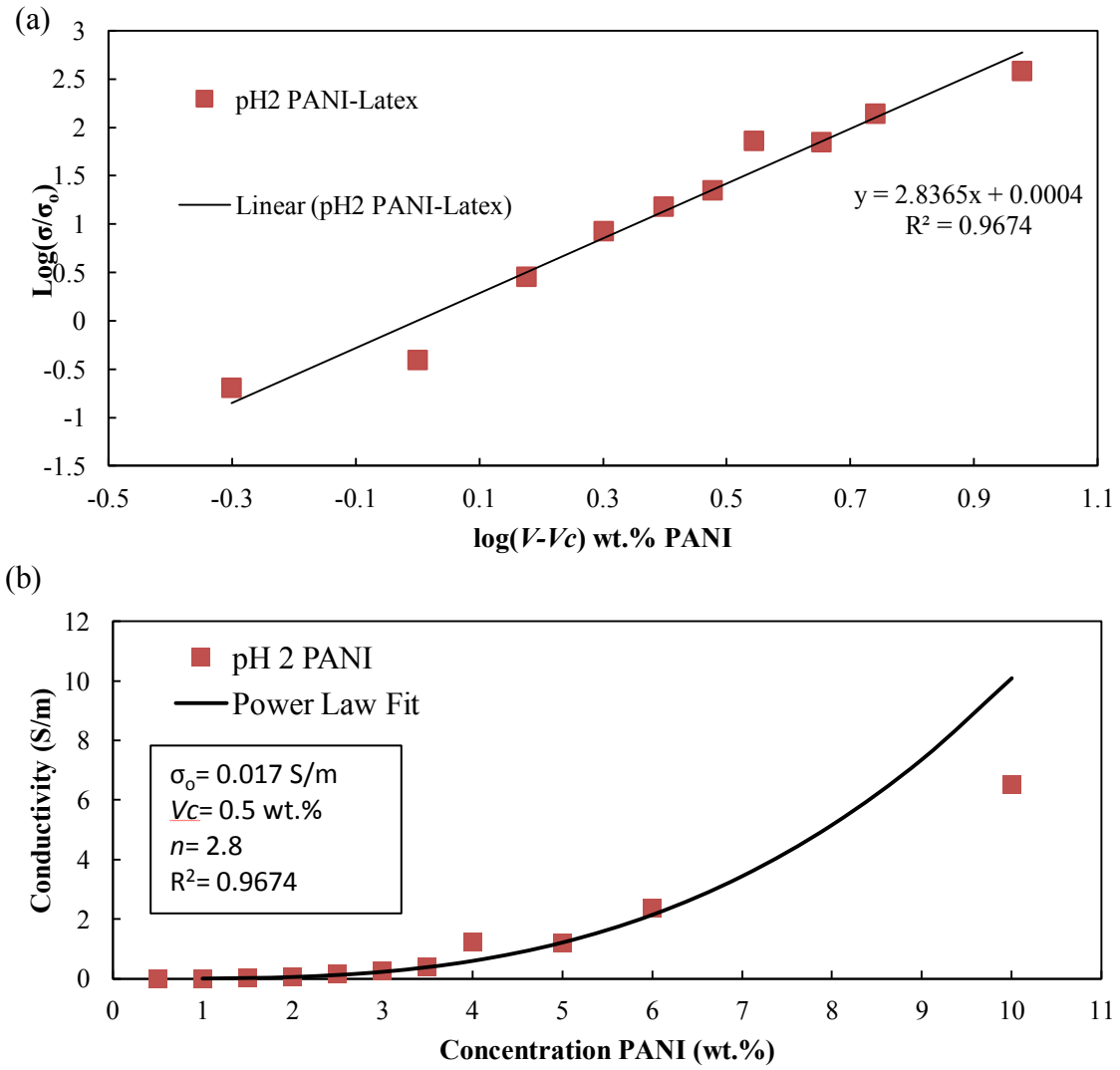

Figure 23. (a) Normalized conductivity as a function of relative concentration of PANI, for pH 2 and 3 PANI-PVAc composites, fitting curve determines power law exponents. (b) Curve overlaying conductivity data and estimated conductivity from power law.

The intrinsic conductivity of the filler in the composite could also be attributed to the phase separation. The existence of separate phases alters the intrinsic conductivity in two ways. First, the existence of regimes with higher concentration of conductive filler will produce an inconsistent calculation of conductivity, due to the unknown dimension

of the conductive segment. The second is the higher concentrations of conductive filler in the conductive regions misrepresent the actual composition. These phase separation are clearly visible when examining the cross section of the composites with the use of SEM, Figure 24.

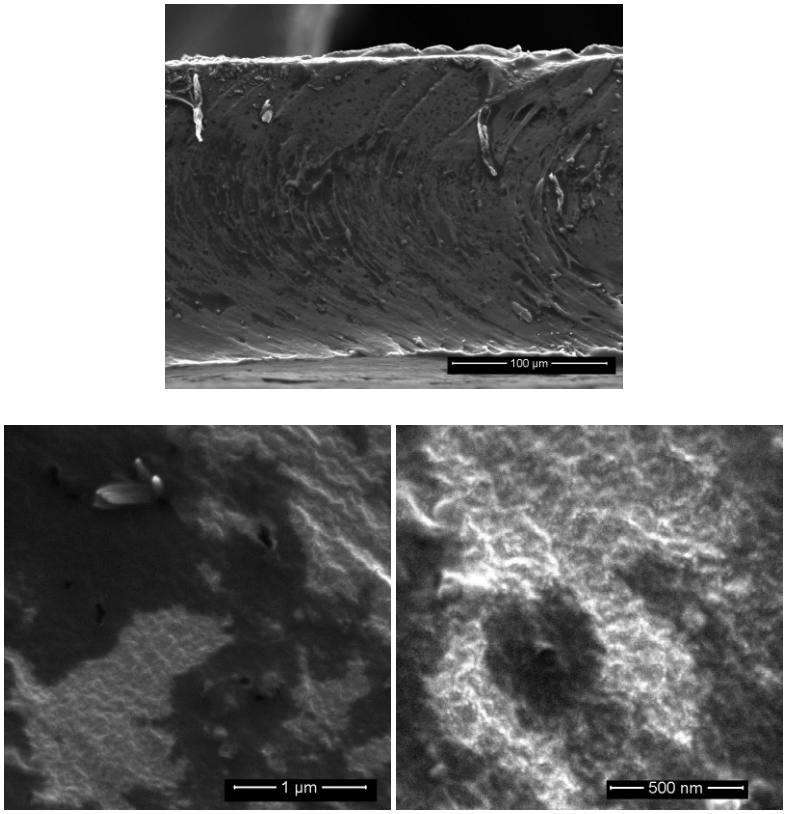

Figure 24. SEM Cross section of pH2 4wt% PANI-Vinnapas copmosite. Lighter regions composed of Latex containing large concentraion of PANI.

The formation of the different regions with varying amounts of PAIN, makes examining the effects of PANI doping difficult. The formation of areas with different concentrations of PANI makes a comparison to system where PANI is evenly dispersed

impossible. These separate regions are likely responsible for the lower geometrical packing constant *n* in the pH 2 series, as the composite consist of a two PANI-Latex regions, one with high PANI concentration and conductivity and low concentration and conductivity.

Conclusions

Altering the filler, matrix composition, and pH has a large influence on the ability of a composite to sense strain. These parameters affect the piezoresistive behavior of the composites in different ways. A more rigid latex material (i.e., higher Tg) shows an improvement over the established PANI-PVAc composites studied in Chapter I, with reduced hysteresis and a more linear response. Despite the improved sensitivity, there is an out of phase response and increased noise for this higher modulus system. Altering the molecular weight of the filler decreases the conductivity of the composites and creates a sensor that does not recover its initial resistance after the load is removed. Higher doped polyaniline creates a composite that phase separates and creates an inhomogeneous composite.

CHAPTER V
SUMMARY AND FUTURE WORK

Summary

Conductive polyaniline-filled polymer composites are complex materials, where differences in the composition can affect the mechanical, electrical, and piezoresistive properties. The composition can be altered in two ways: the composition of the filler or the composition of the matrix material. The filler (i.e., polyaniline) can be altered in several ways: concentration, molecular weight, and level of doping. The composition of the matrix (i.e., latex) can also be altered, by selecting different latex formulations or blending different latexes to tune the mechanical properties. Changing either one can affect the final properties of the composites. The findings of the present work are summarized below, followed by some suggestions about future work.

PANI concentration

Increasing the concentration of filler in a composite increases the conductivity and alters the strain-sensing behavior. Initially the increase PANI concentration forms a more stable network that can better resist fatigue. Increasing the PANI concentration further with reduce the sensitivity and gauge factor of the sensor as the piezoresitive behavior decreases, because the conductive network is to interconnected. The increase

in conductivity with concentration obeys a power law relationship, because the filler is fairly well dispersed throughout the composite. A minimum amount of filler is required to create a conductive network called the percolation threshold and further loading increases the conductivity exponentially until it reaches a maximum value, determined by the conductivity of the filler. The PANI-PVAc composite creates a segregated network of PANI, indicated by the low percolation threshold. The ability to sense strain is not solely based on the conductivity, therefore the effectiveness of a strain sensor cannot be predicted based on the PANI concentration. In general, increasing the amount of filler decreases sensitivity, and attenuation of the signal. Sensors with more PANI have a more repeatable signal with cyclic loading, but the amplitude is smaller than samples with lower concentration. Separation distances of the PANI particles inside the composites are responsible for the strain-sensing behavior. At low concentrations, the same amount of elongation will separate the filler beyond the critical separation distance for electrons to tunnel randomly, disrupting the conductive network. At higher concentrations, more elongation is required to break up the network, reducing the signal amplitude but improving its quality in terms of repeatability, noise, and hysteresis. Based on this research a PANI-Latex Strain sensor would contain between 4-5 wt.% PANI with Vinnapas 401at a pH of 3.

Latex modulus

The composition of the matrix material also affects the conductivity and strain sensing. When the matrix material is more rigid, the percolation threshold of the composite is reduced. The lower percolation threshold is due to inhomogeneous composition of the composites (i.e., polyaniline particles rise to the top surface and create a layer with a high-concentration of conductive filler). An increase in rigid matrix material also causes composites to deform differently than those made with softer materials. The composites deform in an elastic manner, which decreases the amount of hysteresis seen in the loading and unloading response, although the resistance through multiple cycles decreases as defects and cracks form. More flexible composites have a larger hysteresis but are more stable through cycling with less noise.

PANI molecular weight

The molecular weight of the PANI affects the network formed and the movement of the aggregates under elongation. Molecular weight does not seem to affect the size and shape of the basic PANI particles, but particles consisting of higher molecular weight contain loose strands. These loose strands around the particles create better contact with and form a network that has a lower electrical resistance. The higher molecular weight particles also resist separation upon elongation due to the loose strands

anchoring the particles inside the matrix. The anchoring of the particles allows for the change in resistance to be more recoverable.

Doping

The effect of doping the PANI appeared to increase the conductivity of the composites with low concentrations of filler. It was not possible to determine the effect of doping on effective conductivity, because at pH 2 the composites did not form a homogeneous composite so an even comparison cannot be made.

Future work

The two factors that have the most potential to increase the strain-sensing properties of PANI-latex composites are the matrix material and the molecular weight of the filler. The molecular weight of the filler appears to affect the quality of the network formed and the strain sensors durability, and sensitivity. PANI is available in a range of molecular weights and this effect should be studied to determine the relationship between PANI molecular weight, conductivity, and strain sensing. The effects of temperature and strain rate should be examined as these sensors may be used in applications where the strains rates can vary from periods of years to a few seconds. Finally, a study should be conducted to establish if blending different molecular weights

might also improve the strain sensing. Using latex with different mechanical properties (glass transition temperatures, storage modulus, loss modulus) may have the ideal characteristic for good strain sensing. The ideal material would be sufficiently flexible to deform without the formation of defects, yet rigid enough to have low hysteresis. It is possible that no material contains both these properties, so a blend of different latex materials may be considered and should be studied.

REFERENCES

[1] Callister W. Materials Science and Engineering: An Introduction. 7th ed. New York: John Wiley & Sons; 2007:133-43

[2] Beer FP, Johnston ER, DeWolf JT. Mechanics of Materials. 3rd ed. New York: Tata McGraw-Hill; 2006.

[3] Soloman S. Sensors Handbook. New York: McGraw-Hill; 1999.

[4] Bock WJ, Urbanczyk W, Zaremba MB. Electronically scanned white-light interferometric strain sensor employing highly birefringent fibers. Optics Comm 1993;101(3-4):157-62.

[5] Frazao O, Baptista JM, Santos JL, Kobelke J, Schuster K. Sagnac Interferometer based on a Suspended Twin-core Fibre. In: Kalli K, Urbanczyk W, editors. Photonic Crystal Fibers Iv. Bellingham: Spie-Int Soc Optical Engineering; 2010.

[6] Liu CX, Choi JW. Strain-Dependent Resistance of PDMS and Carbon Nanotubes Composite Microstructures. IEEE Trans Nanotechnol 2010;9(5):590-5.

[7] Mohri K, Uchiyama T, Shen LP, Cai CM, Panina LV. Sensitive micro magnetic sensor family utilizing magneto-impedance (MI) and stress-impedance (SI) effects for intelligent measurements and controls. Sensors and Actuators A: Physical 2001;91(1-2):85-90.

[8] Ikeda K, Kuwayama H, Kobayashi T, Watanabe T, Nishikawa T, Yoshida T, et al. Silicon pressure sensor integrates resonant strain gauge on diaphragm. Sensors and Actuators A: Physical 1990;21(1-3):146-50.

[9] Pasquale M. Mechanical sensors and actuators. Sensors Actuat A-Phys 2003;106(1-3):142-8.

[10] Arshak KI, McDonagh D, Durcan MA. Development of new capacitive strain sensors based on thick film polymer and cermet technologies. Sensor Actuat A-Phys 2000;1;79(2):102-14.

[11] Arshak A, Arshak K, Morris D, Korostynska O, Jafer E. Investigation of TiO2 thick film capacitors for use as strain gauge sensors. Sensors Actuat A-Phys 2005;122(2):242-9.

[12] Butler JC, Vigliotti AJ, Verdi FW, Walsh SM. Wireless, passive, resonant-circuit, inductively coupled, inductive strain sensor. Sensors Actuat A-Physical 2002;102(1-2):61-6.

[13] Wilson JS. Sensors Technology Handbook. Wilson JS, editor. Burlington: Elsevier Inc.; 2005.

[14] Yuan L, Ansari F. White-light interferometric fiber-optic distributed strain-sensing system. Sensors Actuat A-Physical. 1997;63(3):177-81.

[15] Tuttle M, Brinson H. Resistance-foil strain-gage technology as applied to composite materials. Exp Mech 1984;24(1):54-65.

[16] Milligan R. The effects of high pressure on foil strain gages. Exp Mech 1964;4(2):25-36.

[17] Milligan R. The effects of high pressure on foil strain gages on convex and concave surfaces. Exp Mech 1965;5(2):59-64.

[18] Cochrane C, Koncar V, Lewandowski M, Dufour C. Design and development of a flexible strain sensor for textile structures based on a conductive polymer composite. Sensors 2007;7(4):473-92.

[19] Lee JC, Lee DW. Flexible and tactile sensor based on a photosensitive polymer. Microelectron Eng 2010;87(5-8):1400-3.

[20] Laukhina E, Pfattner R, Ferreras LR, Galli S, Mas-Torrent M, Masciocchi N, et al. Ultrasensitive piezoresistive all-organic flexible thin films. Adv Mater 2010;22(9):977-81.

[21] Scilingo EP, Gemignani A, Paradiso R, Taccini N, Ghelarducci B, De Rossi D. Performance evaluation of sensing fabrics for monitoring physiological and biomechanical variables. IEEE T Inf Technol Biomed. [Proceedings Paper]. 2005;9(3):345-52.

[22] Feller JF, Grohens Y. Electrical response of poly(styrene)/carbon black conductive polymer composites (CPC) to methanol, toluene, chloroform and styrene vapors as a function of filler nature and matrix tacticity. Synthetic Met 2005;22;154(1-3):193-6.

[23] Omega. Introduction to Strain Gage. Omega Technical Reference. Aug 28, 2011. < http://www.omega.com/prodinfo/straingages.html>

[24] Aizawa S, Kakizawa T, Higasino M. Case studies of smart materials for civil structures. Smart Mater. Struct 1998;7(5):617-26.

[25] Zhou J, Gu YD, Fei P, Mai WJ, Gao YF, Yang RS, et al. Flexible piezotronic strain sensor. Nano Lett. 2008;8(9):3035-40.

[26] Bechtold C, Teliban I, Thede C, Chemnitz S, Quandt E. Non-contact strain measurements based on inverse magnetostriction. Sensors Actuat A-Phys 2010;158(2):224-30.

[27] Ou JP, Han BG. Piezoresistive cement-based strain sensors and self-sensing concrete components. J Intell Mater Syst Struct 2009;20(3):329-36.

[28] Ahmad I, Spiak WA, Janz GJ. Electrodeposition of tantalum and tantalum-chromium alloys. J Appl Electrochem 1981;11(3):291-7.

[29] Benoit JM, Corraze B, Lefrant S, Blau WJ, Bernier P, Chauvet O. Transport properties of PMMA-carbon nanotubes composites. Synthetic Met. [Proceedings Paper]. 2001;121(1-3):1215-6.

[30] Du FM, Scogna RC, Zhou W, Brand S, Fischer JE, Winey KI. Nanotube networks in polymer nanocomposites: Rheology and electrical conductivity. Macromol 2004;37(24):9048-55.

[31] Grunlan JC, Mehrabi AR, Bannon MV, Bahr JL. Water-based single-walled-nanotube-filled polymer composite with an exceptionally low percolation threshold. Adv Mater 2004;16(2):150-3.

[32] Skipina B, Dudic D, Kostoski D, Dojcilovic J. Dielectrical properties of low density polyethylene and carbon black composites. Hem Ind 2010;64(3):187-91.

[33] Mamunya YP, Davydenko VV, Pissis P, Lebedev E. Electrical and thermal conductivity of polymers filled with metal powders. Eur Polym J 2002;38(9):1887-97.

[34] Dyre JC, Schroder TB. Universality of ac conduction in disordered solids. Rev Mod Phys. [Review]. 2000;72(3):873-92.

[35] Hunt A. Approximate power-law conductivity in the multiple-hopping regime. J Non-Cryst Solids 1995;183(1-2):109-21.

[36] Kirkpatrick S. Percolation and conduction. Rev Mod Phys 1973;45(4):574-88.

[37] Adriaanse LJ, Reedijk JA, Teunissen PAA, Brom HB, Michels MAJ, Brokken-Zijp JCM. High-dilution carbon-black/polymer composites: hierarchical percolating network derived from hz to thz ac conductivity. Phys Rev Lett. 1997;78(9):1755-8.

[38] Kim YS, Kim D, Martin KJ, Yu C, Grunlan JC. Influence of stabilizer concentration on transport behavior and thermopower of cnt-filled latex-based composites. Macromol Mater Eng 2010;295(5):431-6.

[39] Yu C, Kim YS, Kim D, Grunlan JC. Thermoelectric behavior of segregated-network polymer nanocomposites. Nano Lett 2008;8(12):4428-32.

[40] Ausanio G, Barone AC, Campana C, Iannotti V, Luponio C, Pepe GP, et al. Giant resistivity change induced by strain in a composite of conducting particles in an elastomer matrix. Sensor Actuat A-Phys 2006;127(1):56-62.

[41] Beruto DT, Capurro M, Marro G. Piezoresistance behavior of silicone-graphite composites in the proximity of the electric percolation threshold. Sensor Actuat A-Phys 2005;117(2):301-8.

[42] Fizazi A, Moulton J, Pakbaz K, Rughooputh SDDV, Smith P, Heeger AJ. Percolation on a self-assembled network - decoration of polyethylene gels with conducting polymer. Phys Rev Lett. 1990;30;64(18):2180-3.

[43] Flandin L, Hiltner A, Baer E. Interrelationships between electrical and mechanical properties of a carbon black-filled ethylene-octene elastomer. Polymer 2001;42(2):827-38.

[44] Chen PF, Adachi K, Kotaka T. Electrical-conductivity of polydiacetylene p(4bcmu) gel .2. a percolation model for elasticity and conductivity. Polymer 1992;33(9):1813-5.

[45] Knite M, Ozols K, Sakale G, Teteris V. Polyisoprene and high structure carbon nanoparticle composite for sensing organic solvent vapours. Sensor Actuat B-Chem. 2007;20;126(1):209-13.

[46] Wang LH, Ding TH, Wang P. Thin flexible pressure sensor array based on carbon black/silicone rubber nanocomposite. IEEE Sensors J 2009;9(9):1130-5.

[47] Knite M, Hill AJ, Pas SJ, Teteris V, Zavickis J. Effects of plasticizer and strain on the percolation threshold in polyisoprene-carbon nanocomposites: positron annihilation lifetime spectroscopy and electrical resistance measurements. Mat Sci Eng C-Bio S. 2006;26(5-7):771-5.

[48] Wright DC, Bergman DJ, Kantor Y. Resistance fluctuations in random resistor networks above and below the percolation-threshold. Phys Rev B. 1986;33(1):396-401.

[49] Hu N, Karube Y, Yan C, Masuda Z, Fukunaga H. Tunneling effect in a polymer/carbon nanotube nanocomposite strain sensor. Acta Mater. 2008;56(13):2929-36.

[50] Knite M, Teteris V, Klemenoks I, Polyakovs B, Erts D. Nanostructure carbon black - polyisoprene composites as prospective strain sensor materials: macro- and nanoscale studies. P Soc Photo-Opt Ins. 2002;4627:113-7334.

[51] Murugaraj P, Mainwaring DE, Mora-Huertas N. Electromechanical response of semiconducting carbon-polyimide nanocomposite thin films. Compos Sci Technol. 2009;69(14):2454-9.

[52] Martin JE, Anderson RA, Odinek J, Adolf D, Williamson J. Controlling percolation in field-structured particle composites: observations of giant thermoresistance, piezoresistance, and chemiresistance. Phys Rev B 2003;67(9).

[53] Aldissi M. Intrinsically conducting polymers: an emerging technology. NATO ASI Series E: Applied Sciences 1992;246:3-6.

[54] Pron A, Rannou P. Processible conjugated polymers: from organic semiconductors to organic metals and superconductors. Prog Polym Sci. [Review] 2002;27(1):135-90.

[55] Roncali J. Molecular engineering of the band gap of pi-conjugated systems: Facing technological applications. Macromol Rapid Comm 2007;28(17):1761-75.

[56] Shirakawa H, Louis EJ, Macdiarmid AG, Chiang CK, Heeger AJ. Synthesis of electrically conducting organic polymers: halogen derivatives of polyacetylene, (ch)x. J Chem Soc Chem Comm 1977(16):578-80.

[57] Tanaka S, Yamashita Y. A novel monomer candidate for intrinsically conductive organic polymers based on nonclassical thiophene. Synthetic Met. 1997;84(1-3):229-30.

[58] Masi JV, New developments in polymers: conductive and active (magnetic, luminescent and electronic) applications. New York: IEEE; 2005.

[59] Skotheim TA. Handbook of Conducting Polymers. 2nd ed. New York: Marcel Dekker INC; 1998.

[60] Plieth W. Electrochemistry for Materials Science. Amsterdam: Elsevier; 2008.

[61] Anand J, Palaniappan S, Sathyanarayana DN. Conducting polyaniline blends and composites. Prog Polym Sci 1998;23(6):993-1018.

[62] Soci C, Hwang IW, Moses D, Zhu Z, Waller D, Gaudiana R, et al. Photoconductivity of a low-bandgap conjugated polymer. Adv Funct Mater 2007;5;17(4):632-6.

[63] Im JS, Kim JG, Lee SH, Lee YS. Enhanced adhesion and dispersion of carbon nanotube in PANI/PEO electrospun fibers for shielding effectiveness of electromagnetic interference. Colloid Surface A 2010l;364(1-3):151-7.

[64] Zukowska G, Zygadlo-Monikowska E, Langwald N, Florjanczyk Z, Borkowska R, Kuzma P, et al. Proton-conducting polymer gels as new materials for electrochemical applications. J New MatElectrochem Syst 2000;3(1):51-4.

[65] Bigg DM, Stutz DE. Plastic composites for electromagnetic-interference shielding applications. Polym Compos 1983;4(1):40-6.

[66] Meyer WH. Polymer electrolytes for lithium-ion batteries. Adv Mater 1998;10(6):439-48.

[67] Somasiri NLD, Macdiarmid AG. Polyaniline: characterization as a cathode active material in rechargeable batteries in aqueous-electrolytes. J Appl Electrochem1988;18(1):92-5.

[68] Brodinova J, Stejskal J, Kalendova A. Investigation of ferrites properties with polyaniline layer in anticorrosive coatings. J Phys Chem Solids [Proceedings Paper] 2007;68(5-6):1091-5.

[69] C. Julien, Pereira-Ramos JP, Momchilov A. New Trends in Intercalation Compounds for Energy Storage. Dordrecht: Kluwer Academic Publishers; 2001.

[70] Michaelson JC. Aniline in history and technology. Endeavour. 1993;17(3):121-6.

[71] Sheibley FE. Carl Julius Fritzsche and the discovery of anthranilic acid, 1841. J Chem Educ 1943;20(3):115.

[72] Anft B. Friedlieb Ferinand Runge: A forgotten chemist of the nineteenth century. J Chem Educ 1955;32(11):566.

[73] Stejskal J, Kratochvíl P, Jenkins AD. The formation of polyaniline and the nature of its structures. Polymer 1996;37(2):367-9.

[74] Stejskal J, Kratochvil P, Jenkins AD. Polyaniline: forms and formation. Collect Czech Chem Commun 1995;60(10):1747-55.

[75] Mu SL, Kong Y, Wu J. Electrochemical polymerization of aniline in phosphoric acid and the properties of polyaniline. Chin J Polym Sci 2004;22(5):405-15.

[76] Duan YP, Wu GL, Li XG, Ji ZJ, Liu SH, Li WP. On the correlation between structural characterization properties of doped polyaniline. Solid State Sci. 2010;12(8):1374-81.

[77] Ponniah D, Xavier F. Electrical and electro reflectance studies on ortho-chloranil-doped polyaniline. Physica B 2007;392(1-2):20-8.

[78] Bacon J, Adams RN. Anodic oxidations of aromatic amines .3. substituted anilines in aqueous media. J Am Chem Soc 1968;90(24):6596-9.

[79] Nekrasov AA, Ivanov VF, Gribkova OL, Vannikov AV. Electrochemical and chemical synthesis of polyaniline on the surface of vacuum deposited polyaniline films. J Electroanal Chem 1996;412(1-2):133-7.

[80] Li GC, Zhang CQ, Li YM, Peng HR, Chen KZ. Rapid polymerization initiated by redox initiator for the synthesis of polyaniline nanofibers. Polymer 2010;51(9):1934-9.

[81] Genies EM, Lapkowski M, Tsintavis C. Preparation, properties and applications of polyaniline. New J Chem [Review]. 1988;12(4):181-96.

[82] Hand RL, Nelson RF. Anodic decomposition pathways of ortho-substituted and meta-substituted anilines. J Electrochem Soc 1978;125(7):1059-69.

[83] Travers JP, Chroboczek J, Devreux F, Genoud F, Nechtschein M, Syed A, et al. Transport and magnetic-resonance studies of polyaniline. Mol Cryst Liq Cryst 1985;121(1-4):195-9.

[84] Macdiarmid AG, Chiang JC, Richter AF, Epstein AJ. Polyaniline - a new concept in conducting polymers. Synthetic Met 1987 Feb;18(1-3):285-90.

[85] Mohilner DM, Argersinger WJ, Adams RN. Investigation of kinetics and mechanism of anodic oxidation of aniline in aqueous sulfuric acid solution at a platinum electrode. J Am Chem Soc 1962;84(19):3618-22.

[86] Diaz AF, Logan JA. Electroactive polyaniline films. J Electroanal Chem 1980;111(1):111-4.

[87] Kitani A, Yano J, Sasaki K. Electrochemical behaviors of electrodeposited poly(n,n-dimethylaniline) - a new organic semiconducting ion-exchange polymer. Chem Lett 1984(9):1565-6.

[88] Wang BC, Tang JS, Wang FS. The effect of anions of supporting electrolyte on the electrochemical polymerization of aniline and the properties of polyaniline. Synthetic Met 1986;13(4):329-34.

[89] Mengoli G, Munari MT, Folonari C. Anodic formation of polynitroanilide films onto copper. J Electroanal Chem 1981;124(1-2):237-46.

[90] Mengoli G, Munari MT, Bianco P, Musiani MM. Anodic synthesis of polyaniline coatings onto Fe sheets. J Appl Polym Sci 1981;26(12):4247-57.

[91] Deberry DW. Modification of the electrochemical and corrosion behavior of stainless-steels with an electroactive coating. J Electrochem Soc 1985;132(5):1022-6.

[92] Oyama N, Ohnuki Y, Chiba K, Ohsaka T. Selectivity of poly(aniline) film-coated electrode for redox reactions of species in solution. Chem Lett 1983(11):1759-62.

[93] Hand RL, Nelson RF. Anodic-oxidation pathways of n-alkylanilines. J Am Chem Soc 1974;96(3):850-60.

[94] Carlin CM, Kepley LJ, Bard AJ. Polymer-films on electrodes .16. Insitu ellipsometric measurements of polybipyrazine, polyaniline, and polyvinylferrocene films. J Electrochem Soc 1985;132(2):353-9.

[95] Singh U, Singh RA. Synthesis and characterization of polyaniline in presence of transition metal salts. Mol Mater 2000;12(1):1-12.

[96] Aurianblajeni B, Taniguchi I, Bockris JO. Photo-electrochemical reduction of carbon-dioxide using polyaniline-coated silicon. J Electroanal Chem [Note] 1983;149(1-2):291-3.

[97] Huang H, Xu JQ, Guo ZC. Synthesis of conducting polyaniline using compound oxidant. In: Ma L, Wang C, Yang W, editors. Advanced Polymer Processing. Stafa-Zurich: Trans Tech Publications Ltd; 2010:300-5.

[98] Tagowska M, Palys B, Jackowska K. Polyaniline nanotubules-anion effect on conformation and oxidation state of polyaniline studied by Raman spectroscopy. Synthetic Met 2004;142(1-3):223-9.

[99] Sacak M, Akbulut U, Batchelder DN. Monitoring of electroinitiated polymerization of aniline by Raman microprobe spectroscopy. Polymer 1999;40(1):21-6.

[100] Chiang JC, Macdiarmid AG. Polyaniline - protonic acid doping of the emeraldine form to the metallic regime. Synthetic Met 1986;13(1-3):193-205.

[101] McCoy CH, Lorkovic IM, Wrighton MS. Potential-dependent nucleophilicity of polyaniline. J Am Chem Soc 1995;117(26):6934-43.

[102] Mattoso LHC, Oliveira ON, Faria RM, Manohar SK, Epstein AJ, Macdiarmid ag. Synthesis of polyaniline polytoluidine block-copolymer via the pernigraniline oxidation-state. Polym Int 1994;35(1):89-93.

[103] Epstein AJ, Ginder JM, Zuo F, Bigelow RW, Woo HS, Tanner DB, et al. Insulator-to-metal transition in polyaniline. Synthetic Met 1987;18(1-3):303-9.

[104] Cao Y, Smith P, Heeger AJ. Counterion induced processibility of conducting polyaniline and of conducting polyblends of polyaniline in bulk polymers. Synthetic Met 1992;48(1):91-7.

[105] Stejskal J, Gilbert RG. Polyaniline: preparation of a conducting polymer (IUPAC technical report). Pure Appl Chem 2002;74(5):857-67.

[106] Liu W, Kumar J, Tripathy S, Senecal KJ, Samuelson L. Enzymatically synthesized conducting polyaniline. J Am Chem Soc 1999;121(1):71-8.

[107] Palaniappan S, Amarnath CA. A novel polyaniline-maleicacid-dodecylhydrogensulfate salt: soluble polyaniline powder. React Funct Polym 2006;66(12):1741-8.

[108] Angelopoulos M, Ermer SP, Manohar SK, Macdiarmid AG, Epstein AJ. Pseudo-protonic acid doping of polyaniline. Mol Cryst Liq Cryst 1988;160:223.

109] Cao Y. Spectroscopic studies of acceptor and donor doping of polyaniline in the emeraldine base and pernigraniline forms. Synthetic Met 1990;35(3):319-32.

[110] Macdiarmid AG, Epstein AJ. New developments in the synthesis and doping of polyacetylene and polyaniline. Nato Adv Sci I E-App 1990;182:53-63.

[111] Macdiarmid AG, Epstein AJ. Secondary doping in polyaniline. Synthetic Met 1995;69(1-3):85-92.

[112] Macdiarmid AG, Epstein AJ. Synthetic metals: a novel role for organic polymers. P IEEE Embs 1989;11:1299.

[113] Liu H, Hu XB, Wang JY, Boughton RI. Structure, conductivity, and thermopower of crystalline polyaniline synthesized by the ultrasonic irradiation polymerization method. Macromol 2002;35(25):9414-9.

[114] Cromack KR, Jozefowicz ME, Ginder JM, Epstein AJ, McCall RP, Du G, et al. Thermal process for orientation of polyaniline films. Macromol 1991;24(14):4157-61.

[115] Abell L, Devasagayam P, Adams PN, Monkman AP, Soc Plast E. Crystallinity and stretch orientation in polyaniline camphor-sulphonic acid films. Brookfield Center: Soc Plastics Engineers; 1997.

[116] Oh EJ, Min Y, Wiesinger JM, Manohar SK, Scherr EM, Prest PJ, et al. polyaniline: dependency of selected properties on molecular-weight. Synthetic Met [Proceedings Paper]. 1993;55(2-3):977-82.

[117] Song JX, Han DX, Li F, Niu L. Preparations of nano/micro structured polyaniline membranes for ph sensing. Chem J Chin Univ-Chin 2010;31(8):1688-92.

[118] Cho S, Seo JH, Kim SH, Song S, Jin Y, Lee K, et al. Effect of substituted side chain on donor-acceptor conjugated copolymers. Appl Phys Lett. 2008; 29;93(26):263301-3.

[119] Wang X, Sun TL, Wang CY, Wang C, Zhang WJ, Wei Y. H-1 nmr determination of the doping level of doped polyaniline. Macromol Chem Phys 2010;211(16):1814-9.

[120] Ngo TT, Lee H, Song Y, Nguyen DN, Sohn D. Structure and properties of selenious acid doped polyaniline with varied dopant content. Synthetic Met 2010;160(11-12):1303-6.

[121] Genies EM, Boyle A, Lapkowski M, Tsintavis C. Polyaniline: a historical survey. Synthetic Met 1990;36(2):139-82.

[122] Chakraborty G, Guatak S, Meikap AK, Woods T, Babu R, Blau WJ. Characterization and electrical transport properties of polyaniline and multiwall carbon nanotube composites. J Polym Sci Pol Phys 2010;48(15):1767-75.

[123] Zou WY, Wang W, He BL, Sun ML, Wang M, Liu L, et al. Effects of counterions on pseudocapacitance performance of polyaniline in sulfuric acid and p-toluene sulphonic acid electrolyte. J Electroanal Chem 2010;641(1-2):111-8.

[124] Wang X, Bernard MC, Deslouis C, Joiret S, Rousseau P. A new transfer function in electrochemistry: Dynamic coupling between Raman spectroscopy and electrochemical impedance spectroscopy. Electrochim Acta 2010;55(21):6299-307.

[125] Izumi CMS, Brito HF, Ferreira A, Constantino VRL, Temperini MLA. Spectroscopic investigation of the interactions between emeraldine base polyaniline and Eu(III) ions. Synthetic Met 2009;159(5-6):377-84.

[126] da Silva JEP, Temperini MLA, de Torresi SIC. Secondary doping of polyaniline studied by resonance Raman spectroscopy. Electrochim Acta 1999;44(12):1887-91.

[127] Gruger A, Novak A, Regis A, Colomban P. Infrared and raman-study of polyaniline .2. Influence of ortho substituents on hydrogen-bonding and uv/vis near-ir electron charge-transfer. J Mol Struct 1994;328:153-67.

[128] Huang WS, Macdiarmid AG. Optical-properties of polyaniline. Polymer 1993;34(9):1833-45.

[129] Pratt FL, Blundell SJ, Hayes W, Nagamine K, Ishida K, Monkman AP. Anisotropic polaron motion in polyaniline studied by muon spin relaxation. Phys Rev Lett 1997;79(15):2855-8.

[130] Kapil A, Taunk M, Chand S. Preparation and charge transport studies of chemically synthesized polyaniline. J Mater Sci-Mater Electron 2010;21(4):399-404.

[131] Wnek GE. A proposal for the mechanism of conduction in polyaniline. Synthetic Met.1986;15(2-3):213-8.

[132] Cheung JH, Fou AF, Rubner MF. Molecular self-assembly of conducting polymers. Thin Solid Films 1994;244(1-2):985-9.

[133] Chartoff R, Weissman P, Sircar A. The application of dynamic mechanical methods to tg determination in polymers: an overview. ASTM STP. 1994;1249.

[134] Kota AK, Cipriano BH, Duesterberg MK, Gershon AL, Powell D, Raghavan SR, et al. Electrical and rheological percolation in polystyrene/MWCNT nanocomposites. Macromol 2007;40(20):7400-6.

[135] Chapartegui M, Markaide N, Florez S, Elizetxea C, Fernandez M, Santamaria A. Specific rheological and electrical features of carbon nanotube dispersions in an epoxy matrix. Compos Sci Technol 2010;70(5):879-84.

[136] Abbasi S, Carreau PJ, Derdouri A. Flow induced orientation of multiwalled carbon nanotubes in polycarbonate nanocomposites: Rheology, conductivity and mechanical properties. Polymer 2010;51(4):922-35.

[137] Potschke P, Abdel-Goad M, Pegel S, Jehnichen D, Mark JE, Zhou DH, et al. Comparisons among electrical and rheological properties of melt-mixed composites containing various carbon nanostructures. J Macromol Sci Part A-Pure Appl Chem 2010;47(1):12-9.

[138] Roldughin VI, Vysotskii VV. Percolation properties of metal-filled polymer films, structure and mechanisms of conductivity. Progress Org Coat 2000;39(2-4):81-100.

[139] Barkauskas J, Vinslovaite A. Investigation of electroconductive films composed of polyvinyl alcohol and graphitized carbon black. Mater Res Bull 2003;38(8):1437-47.

[140] Grady BP, Paul A, Peters JE, Ford WT. Glass transition behavior of single-walled carbon nanotube-polystyrene composites. Macromol 2009;42(16):6152-8.

[141] Xu J, Razeeb KM, Roy S. Thermal properties of single walled carbon nanotube-silicone nanocomposites. J Polym Sci Pol Phys 2008;46(17):1845-52.

[142] Grossiord N, Miltner HE, Loos J, Meuldijk J, Van Mele B, Koning CE. On the crucial role of wetting in the preparation of conductive polystyrene-carbon nanotube composites. Chem Mater 2007;19(15):3787-92.

[143] Segal E, Haba Y, Narkis M, Siegmann A. On the structure and electrical conductivity of polyaniline/polystyrene blends prepared by an aqueous-dispersion blending method. J Polym Sci Pol Phys 2001;39(5):611-21.

VITA

Name:	Zachary Solomon Levin
Address:	Department of Mechanical Engineering, Room 100 3123 ENPH College Station TX 77841.
Email Address:	ZachSLevin@gmail.com
Education:	B.S. Engineering Physics, New Mexico State University, Las Cruces, New Mexico, May 2008
	M.S. Mechanical Engineering, Texas A&M University, College Station, Texas, December 2011